

**NJC**

Probing the effect of arm length and inter- and intramolecular interactions in the formation of Cu(II) complexes of Schiff base ligands derived from some unsymmetrical tripodal amines

Journal:	<i>New Journal of Chemistry</i>
Manuscript ID:	NJ-ART-05-2015-001318.R1
Article Type:	Paper
Date Submitted by the Author:	13-Jul-2015
Complete List of Authors:	Keypour, Hassan; university , chemistry Shayesteh, Maryam; university, chemistry Salehzadeh, Sadegh; university, chemistry Dhers, Sebastien; Laboratoire de Chimie de Coordination du CNRS, Maleki, Farahnaz; university, chemistry Ünver, Hüseyin; university, Physics Dilek, Nefise; university, Physics

SCHOLARONE™
Manuscripts

Cite this: DOI: 10.1039/c0xx00000x

FULL PAPER

www.rsc.org/xxxxxx

Probing the effect of arm length and inter- and intramolecular interactions in the formation of Cu(II) complexes of Schiff base ligands derived from some unsymmetrical tripodal amines

Hassan Keypour,^a * Maryam Shayesteh,^a Sadegh Salehzadeh,^a Sébastien Dhers,^b Farahnaz Maleki,^a Hüseyin Ünver^c and Nefise Dilek^d

Received (in XXX, XXX) Xth XXXXXXXXXX 20XX, Accepted Xth XXXXXXXXXX 20XX

DOI: 10.1039/b000000x

The syntheses of two previously known, 2-((2-aminoethyl)(pyridin-2-ylmethyl)amino)ethanol (**1**) and 2-((3-aminopropyl)(pyridin-2-ylmethyl)amino)ethanol (**2**) and four new unsymmetrical N-capped tripodal amines, 2-((4-aminobutyl)(pyridin-2-ylmethyl)amino)ethanol (**3**), 3-((2-aminoethyl)(pyridin-2-ylmethyl)amino)propan-1-ol (**4**), 3-((3-aminopropyl)(pyridin-2-ylmethyl)amino)propan-1-ol (**5**) and 3-((4-aminobutyl)(pyridin-2-ylmethyl)amino)propan-1-ol (**6**) are reported. The ligands (**3**)-(4) feature a longer arm, 3-hydroxypropyl or butylamino, than in the analogues previously employed (2-hydroxyethyl arm, ethylamino-arm or propylamino-arm in **1** and **2**). All six tripodal amines, **1-6**, are equipped with a 2-methylpyridyl-arm and either an ethylamino-arm (**1** and **4**), propylamino-arm (**2** and **5**) or butylamino-arm (**3** and **6**). The new amines, **3-6**, have been employed in one pot condensation reactions with 2-hydroxy-1-naphthaldehyde and salicylaldehyde (and its derivatives) in the presence of Cu(II) metal ion to generate a series of new mononuclear complexes, $[M^{II}L^{ald}](ClO_4)$ as well as new dinuclear complexes $[Cu^{II}L^{ald}]_2(ClO_4)_2$ of new ligands L^{ald} . Four monomeric complexes and one dimeric complex have been characterised by single crystal X-ray diffraction, revealing a distorted square-pyramidal copper(II) ion. A general comparison between these structures show that the number and the type of chelate rings sequence around the metal ions are important in the formation of structures. Theoretical studies show that the 3-hydroxypropyl arm in these complexes is a weak coordinating group and it can readily be removed from the coordination sphere of metal ion, resulting in a dimerised four coordinate complex. Calculations show that the interaction between the two monomeric fragments is very weak.

Introduction

Recently, research on tripodal ligands and their related complexes has been an expanding field and is the subject of numerous reports.¹ Transition metal complexes synthesised with this type of ligand display special physical, chemical or structural properties, such as unusual conformation, high thermodynamic stability and virtual kinetic inertness.² These tripodal ligands can also serve as precursors to the synthesis of interesting macrobicyclic compounds^{3,4} which usually require high dilution techniques⁵ or the use of metal ions as templates.^{6,7} The synthesis of model complexes mimicking the spectroscopic and structural properties of metalloproteins active sites can be undertaken by employing multidentate tripodal ligands, most of which possess aromatic donor functions like pyridyl and/or phenolic groups.⁸ However, the chemistry of asymmetric N-capped tripodal ligands which possess three pendant arms with different donor groups has not been well explored.^{9,10} This type of tripodal ligand is of particular

interest in the context of modeling the asymmetric active metal sites such as those found in nitrile hydratase,¹¹ and horse liver alcohol dehydrogenase.¹² Among these asymmetric N-capped tripodal ligands, our group is particularly interested in unsymmetric N-capped tripodal ligands with two different aliphatic arm lengths and one aromatic pendant arm. However these tripodal ligands bearing one pyridine arm are scarce.¹³ As part of a program to explore the coordination chemistry of partially unsymmetric tripodal N_3O_2 ligands, we herein report the synthesis and characterisation of new Cu complexes and compare them with our previous work. A direct influence of the lengths of the alkyl chains between central and terminal donor function on the complex geometry was observed for the cadmium(II), nickel(II) and copper(II) complexes of these unsymmetrical tripodal ligands featuring different spacer lengths (Fig. 1). The coordination behavior towards Cd(II), Ni(II) and Cu(II) was investigated for ligands L^{ald} combining pyridine, amine, and alkoxy donor functions on ethylene, propylene and butylene spacers.¹⁴

In previous work, we reported the synthesis of two new unsymmetrical triamines, (1) and (2), both of which feature three different arms: 2-methylpyridyl, either ethylamino- or propylamino, and ethanol (Figure 1).¹⁴ Reaction of (1) or (2) with salicylaldehyde and its analogues gave a wide selection of compounds with which to probe the effects of strain in the resulting cadmium(II) and nickel(II) Schiff base complexes (Figure 1).¹⁴ When the shorter ethylene linker was used between the tertiary and primary amine nitrogen atoms, a mononuclear Schiff base complex was structurally characterised in the case of [Ni^{II}L^{OMe1}]⁺ whereas the more flexible propylene linker (L^{OMe2} and L^{H2} ligands) gave dinuclear complexes, [Ni^{II}L^{OMe2}]₂²⁺ and [Cd^{II}L^{H2}]₂²⁺, which were structurally characterised. The nickel(II) centre in [Ni^{II}L^{OMe1}]⁺ has a distorted square planar geometry, whereas in [Ni^{II}L^{OMe2}]₂²⁺ the geometry is distorted octahedral, as with the cadmium(II) ion in [Cd^{II}L^{H2}]₂²⁺.¹⁴ The structural types observed to date are summarised in Figure 1.

In this paper the effect of employing a 3-hydroxypropyl arm in place of the 2-hydroxyethyl arm, and a butylamino arm in place

of the ethylamino or propylamino arm, on the outcome of one pot condensations with various salicylaldehydes in the presence of copper(II) ion has been studied. Hence the synthesis of four new unsymmetrical tripodal triamines, 2-((4-aminobutyl)(pyridin-2-ylmethyl)amino)ethanol (3), 3-((2-aminoethyl)(pyridin-2-ylmethyl)amino)propan-1-ol (4), 3-((3-aminopropyl)(pyridin-2-ylmethyl)amino)propan-1-ol (5) or 3-((4-aminobutyl)(pyridin-2-ylmethyl)amino)propan-1-ol (6), is reported (Figure 1). The synthesis and physical properties of the new Cu(II) complexes of the new ligands, HL^{H3-6}, HL^{OMe3-6} and HL^{tBu3-6} formed in situ from the condensation of 2-hydroxybenzaldehyde with 3-6 (HL^{H3-6}), 2-hydroxy-3-methoxy-benzaldehyde with 3-6 (HL^{OMe3-6}), 3,5-di-tert-butylsalicylaldehyde with 3-6 (HL^{tBu3-6}) and, for the first time, with 2-hydroxy-1-naphthaldehyde with 1-6 (HL^{naph1-6}), are reported here. In addition, the X-ray crystal structures of [Cu^{II}L^{naph2}](ClO₄), [Cu^{II}L^{OMe3}](ClO₄), [Cu^{II}L^{H3}](ClO₄), [Cu^{II}L^{H4}](ClO₄) and dimeric [Cu^{II}L^{H5}]₂(ClO₄)₂, are described.

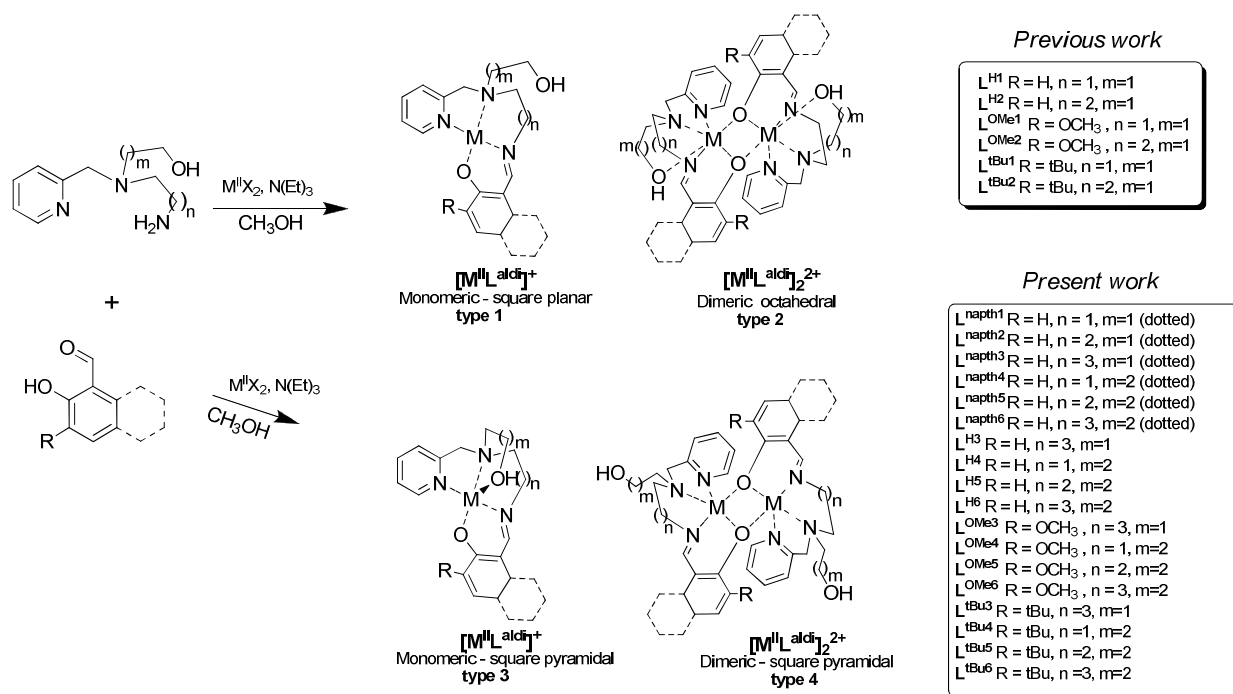


Figure 1. Summary of the range of structural motifs identified to date for complexes resulting from the condensation of a range of salicylaldehydes with the unsymmetrical triamines 1 (n = 1, m = 1) and 2 (n = 2, m = 1) with 2-hydroxyethyl arms but differing amino-arm lengths. The present study concerns complexes of the new ligands highlighted in the box, HL^{H3-6}, HL^{OMe3-6}, HL^{tBu3-6} and HL^{naph1-6} (X = ClO₄).

Results and discussion

Four new unsymmetrical tripodal amines, 2-((4-aminobutyl)(pyridin-2-ylmethyl)amino)ethanol (3), 3-((2-aminoethyl)(pyridin-2-ylmethyl)amino)propan-1-ol (4), 3-((3-aminopropyl)(pyridin-2-ylmethyl)amino)propan-1-ol (5) and 3-((4-aminobutyl)(pyridin-2-ylmethyl)amino)propan-1-ol (6), were prepared in high yields. Amines 3 - 6 differ from the previously used amines, 1 and 2, in that 4 and 5 feature a 3-hydroxypropyl arm in place of the 2-hydroxyethyl arm, 3 features a butylamino arm in place of the ethylamino/propylamino arm and 6 features a 3-hydroxypropyl arm in place of the 2-hydroxyethyl arm and also a butylamino arm in place of the ethylamino/propylamino arm

(Fig. S1–S12, ESI[†]). Subsequently, one pot reactions of amines 1 - 6 with 2-hydroxy-1-naphthaldehyde and salicylaldehyde derivatives in the presence of a Cu(II) metal salt were employed to generate new Cu(II) complexes of Schiff-base ligands L^{aldi}, where ^{aldi} is H3-6, OMe3-6, tBu3-6 and naph1-6 (Figure 1). Recrystallisation of powders obtained from the reaction mixture by vapour diffusion of diethyl ether (see experimental section below) gave either purified powders or single crystals which were analysed by single crystal X-ray diffraction, showing four monomeric and one dimeric compounds (*vide infra*).

The infrared spectra of all complexes (Fig. S13–S30, ESI[†]) show a band at ca. 1613–1632 cm⁻¹, attributable to the imine groups, and no bands due to ν(C=O) vibrations. Medium to strong bands

at ca. 1596–1612 and 1437–1462 cm^{-1} are present in all cases, and correspond to the two highest energy ring vibrations of the coordinated pyridine.^{14,15} Absorptions attributable to the perchlorate ions are seen at approximately 1051–1088 and 619–625 cm^{-1} . The lack of splitting suggests that they are not coordinated.

The positive ion electrospray mass spectra of all complexes (Fig. S31–S48, ESI⁺) show a common peak, which is the fragment $[\text{Cu}^{\text{II}}\text{L}^{\text{ald}}]^+$ associated with the loss of the ClO_4^- anion. The four copper(II) complexes using $(\text{L}^{\text{ald}})^-$ as a ligand appear to be dimeric complexes $[\text{Cu}^{\text{II}}\text{L}^{\text{ald}}]_2(\text{ClO}_4)_2$ as the mass spectra exhibit peaks of very weak intensity consistent with the presence of a dication $[\text{CuL}^{\text{ald}}]_2^{2+}$. In all copper(II) complexes the most intense peaks are for the mononuclear $[\text{Cu}^{\text{II}}\text{L}^{\text{ald}}]^+$ species which indicates that the dimer is unsurprisingly broken apart. On the other hand, a peak with a very weak intensity corresponds to $[\text{ML}^{\text{ald}}]_2^+$ fragment is observed in most of the mononuclear complexes in present work and also in our previous work,¹⁴ even when their X-ray crystal structures show that they are mononuclear complexes. Thus it seems that the $[\text{ML}^{\text{ald}}]_2^+$ fragment observed in the mass spectra of the mononuclear complexes is formed due to a very small dimerization occurring in the mass spectrometer.

UV-Vis spectra of the fourteen Cu(II) complexes in CH_3CN solution showed a broad low-intensity absorption band occurring in the range $574 \text{ nm} < \lambda_{\text{max}} < 630 \text{ nm}$ with molar extinction coefficient ranging between $92 \text{ M}^{-1} \text{ cm}^{-1} < \epsilon < 174 \text{ M}^{-1} \text{ cm}^{-1}$. This is assigned to a d–d transition and is characteristic of five-coordinate copper(II) complexes with square pyramidal or distorted square pyramidal geometries, which generally exhibit a band in the 550–660 nm range ($\text{dx}_z, \text{dy}_z \rightarrow \text{dx}^2 - \text{y}^2$).^{16–24} In the case of four Cu complexes $[\text{Cu}^{\text{II}}\text{L}^{\text{ald}}]\text{ClO}_4$ ($i=3$), the respective λ_{max} values in the range $600 \text{ nm} < \lambda_{\text{max}} < 633 \text{ nm}$ and $121 \text{ M}^{-1} \text{ cm}^{-1} < \epsilon < 157 \text{ M}^{-1} \text{ cm}^{-1}$ (each with a shoulder at 761–819 nm) are also indicative of square-pyramidal coordination according to the literature.^{25,26} In addition, a few absorption bands are found in the range 205–406 nm for all Cu(II) complexes, due to either charge transfer or $\pi-\pi^*$ transitions.^{19, 21, 27–29} Although the UV-Vis spectra of complexes with polydentate Schiff base ligands are not generally good indicators of geometry, the evidence gathered helps to support this geometry.

Room temperature magnetic moments were obtained for all mononuclear Cu(II) complexes. The magnetic moment values for these complexes lie in the 1.82–1.95 B.M. range. These values are close to the expected spin only magnetic moment value (1.73 BM) for d^9 Cu(II) system³⁰ with single unpaired electron. For the four dinuclear copper complexes, the observed values of magnetic moment lie in the 1.32–1.66 BM range per Cu atom.

Crystal structures of $[\text{Cu}^{\text{II}}\text{L}^{\text{naph}}]_2(\text{ClO}_4)_2$, $[\text{Cu}^{\text{II}}\text{L}^{\text{H}3}]\text{ClO}_4$, $[\text{Cu}^{\text{II}}\text{L}^{\text{OMe}3}]\text{ClO}_4$ and $[\text{Cu}^{\text{II}}\text{L}^{\text{H}4}]\text{ClO}_4$

Green single crystals of $[\text{Cu}^{\text{II}}\text{L}^{\text{naph}}]_2(\text{ClO}_4)_2$, $[\text{Cu}^{\text{II}}\text{L}^{\text{H}3}]\text{ClO}_4$, $[\text{Cu}^{\text{II}}\text{L}^{\text{OMe}3}]\text{ClO}_4$ and $[\text{Cu}^{\text{II}}\text{L}^{\text{H}4}]\text{ClO}_4$ suitable to be studied by X-ray diffraction were obtained by slow diffusion of diethyl ether into a solution of the complex in MeOH. Crystal data and structure refinement are given in Table 1. These complexes are monometallic but differ in the space group adopted ($P2_1/c$, $C2/c$, $P-1$ and $I2/a$ respectively). The molecular structures, as well as selected bond lengths and angles are given in Figure 2 and Table 2, respectively, and a comparison with the literature is also

shown. The X-ray crystal structures of these complexes consist of $[\text{Cu}^{\text{II}}\text{L}^{\text{naph}}]_2^+$, $[\text{Cu}^{\text{II}}\text{L}^{\text{H}3}]^+$, $[\text{Cu}^{\text{II}}\text{L}^{\text{OMe}3}]^+$ and $[\text{Cu}^{\text{II}}\text{L}^{\text{H}4}]^+$ cations and perchlorate anion. The Cu(II) ion display a distorted square pyramidal coordination, involving three N atoms and two O atoms. In comparison to the mononuclear $[\text{Ni}^{\text{II}}\text{L}^{\text{OMe}1}]\text{ClO}_4$ complex reported in our previous work,¹⁴ in which the hydroxyl group is not coordinated, in these mononuclear copper(II) complexes it is coordinated to the apical site of the approximate square pyramidal copper(II) ion (Table 2). As expected, this axially bound O donor atom makes a bond that is slightly longer than bond distances in basal plane ($\sim 2 \text{ \AA}$). Among the Cu-N bonds, those involving the tertiary amine nitrogen atoms are the longest in all Cu complexes. The second longest Cu-N bond formed in both mononuclear and dinuclear complexes involves the Cu- N_{py} bonds. Comparison of the same bond lengths of square pyramidal Cu(II) complexes reported here with related reports in the literature are summarised in Table 2.^{14, 19, 31–38} The X-ray crystal structure analysis shows that in the case of $[\text{Cu}^{\text{II}}\text{L}^{\text{OMe}3}]\text{ClO}_4$, two $[\text{Cu}^{\text{II}}\text{L}^{\text{OMe}3}]^+$ cations are bonded through hydrogen bonding. Indeed, the hydrogen atom of the hydroxyl group of one cation is engaged in hydrogen bonding with the phenolic oxygen atom of the adjacent cation and vice versa (Fig. 5a). It seems that these intermolecular interactions between two molecules of such five coordinate complex in $[\text{Cu}^{\text{II}}\text{L}^{\text{OMe}3}]\text{ClO}_4$ are relatively strong and prevent the formation of dinuclear compounds (see section theoretical studies). Note that the dataset for $[\text{Cu}^{\text{II}}\text{L}^{\text{OMe}3}]\text{ClO}_4$ was particularly bad, leading to a high R1 factor, this despite our best efforts to grow better crystals - the results presented here are from the best dataset obtained.

Variation of the length of the ligand arms leads to different size of chelate rings. These tripodal ligands are capable of forming both five and six membered chelate rings incorporating the copper ion in $[\text{Cu}^{\text{II}}\text{L}^{\text{naph}}]_2(\text{ClO}_4)_2$, $[\text{Cu}^{\text{II}}\text{L}^{\text{H}4}]\text{ClO}_4$ and $[\text{Cu}^{\text{II}}\text{L}^{\text{H}5}]_2(\text{ClO}_4)_2$ and also five, six and seven membered chelate rings in $[\text{Cu}^{\text{II}}\text{L}^{\text{H}3}]\text{ClO}_4$ and $[\text{Cu}^{\text{II}}\text{L}^{\text{OMe}3}]\text{ClO}_4$. For all complexes, the $\text{N}_{\text{amine}}\text{-Cu-}\text{N}_{\text{py}}$ angles are smaller than 90° [$80.5\text{--}84.3^\circ$] for five membered chelate rings. The larger six-membered chelate rings lead to $\text{O}_{\text{phenolic}}\text{-Cu-}\text{N}_{\text{imine}}$ angles that are all larger than 90° [$90.2\text{--}94.5^\circ$]. A similar relationship between the $\text{N}_{\text{amine}}\text{-Cu-}\text{O}_{\text{hydroxyalkyl}}$ and also $\text{N}_{\text{amine}}\text{-Cu-}\text{N}_{\text{imine}}$ angles and the different chelate ring sizes is described. In the case of $[\text{Cu}^{\text{II}}\text{L}^{\text{naph}}]_2(\text{ClO}_4)_2$, $[\text{Cu}^{\text{II}}\text{L}^{\text{H}3}]\text{ClO}_4$ and $[\text{Cu}^{\text{II}}\text{L}^{\text{OMe}3}]\text{ClO}_4$ complexes, involving the 2-hydroxyethyl arm, the $\text{N}_{\text{amine}}\text{-Cu-}\text{O}_{\text{hydroxyalkyl}}$ angles are smaller than 90° [$78.6\text{--}80.9^\circ$] for five membered chelate rings, whilst in $[\text{Cu}^{\text{II}}\text{L}^{\text{H}4}]\text{ClO}_4$ complex involving the 3-hydroxypropyl arm, the $\text{N}_{\text{amine}}\text{-Cu-}\text{O}_{\text{hydroxyalkyl}}$ angle is $\sim 90^\circ$ [89.27°] for the six-membered ring. The $\text{N}_{\text{amine}}\text{-Cu-}\text{N}_{\text{imine}}$ angle in $[\text{Cu}^{\text{II}}\text{L}^{\text{H}4}]\text{ClO}_4$, involving the ethylamine chain [86.37°] is smaller than 90° for five membered chelate ring, in $[\text{Cu}^{\text{II}}\text{L}^{\text{naph}}]_2(\text{ClO}_4)_2$ and $[\text{Cu}^{\text{II}}\text{L}^{\text{H}5}]_2(\text{ClO}_4)_2$ complexes, involving the propylamine chain [$94.2\text{--}96.2^\circ$] and also in $[\text{Cu}^{\text{II}}\text{L}^{\text{H}3}]\text{ClO}_4$ and $[\text{Cu}^{\text{II}}\text{L}^{\text{OMe}3}]\text{ClO}_4$ complexes, involving the butylamine chain [$102.9\text{--}104.0^\circ$] are larger than 90° for six and seven membered chelate rings, respectively (Table 2). The square pyramid in Cu complexes is somewhat trigonally distorted, as shown by the degree of trigonality, (τ)^{39–41} for Cu(1) being 0.10, 0.11, 0.066 and 0.39 for $[\text{Cu}^{\text{II}}\text{L}^{\text{naph}}]_2(\text{ClO}_4)_2$, $[\text{Cu}^{\text{II}}\text{L}^{\text{H}3}]\text{ClO}_4$, $[\text{Cu}^{\text{II}}\text{L}^{\text{OMe}3}]\text{ClO}_4$ and $[\text{Cu}^{\text{II}}\text{L}^{\text{H}4}]\text{ClO}_4$, respectively.

Cite this: DOI: 10.1039/c0xx00000x

www.rsc.org/xxxxxx

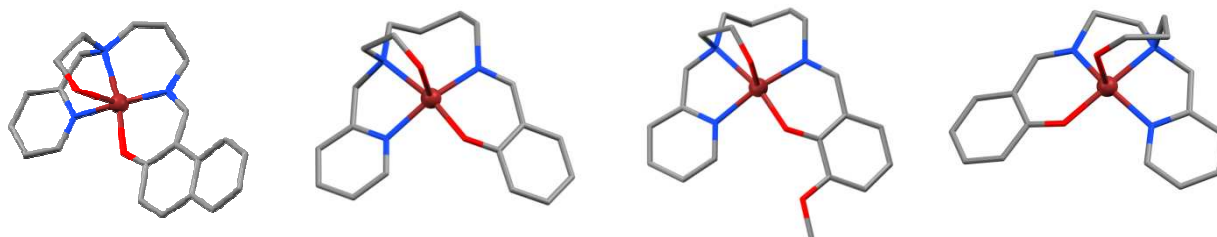


Figure 2. Perspective view of (from left to right) $[\text{Cu}^{\text{II}}\text{L}^{\text{naph}2}](\text{ClO}_4)$, $[\text{Cu}^{\text{II}}\text{L}^{\text{H}3}](\text{ClO}_4)$, $[\text{Cu}^{\text{II}}\text{L}^{\text{OMe}3}](\text{ClO}_4)$ and $[\text{Cu}^{\text{II}}\text{L}^{\text{H}4}](\text{ClO}_4)$. Hydrogen atoms and anions are omitted for clarity. Cu, C, N and O are represented in dark red, gray, blue and red, respectively.

Table 1. Crystal data and structure refinement parameters for $[\text{Cu}^{\text{II}}\text{L}^{\text{naph}2}](\text{ClO}_4)$, $[\text{Cu}^{\text{II}}\text{L}^{\text{H}3}](\text{ClO}_4)$, $[\text{Cu}^{\text{II}}\text{L}^{\text{OMe}3}](\text{ClO}_4)$, $[\text{Cu}^{\text{II}}\text{L}^{\text{H}4}](\text{ClO}_4)$ and $[\text{Cu}^{\text{II}}\text{L}^{\text{H}5}]_2(\text{ClO}_4)_2$.

Compound formula	$[\text{Cu}^{\text{II}}\text{L}^{\text{naph}2}](\text{ClO}_4)$ $\text{C}_{22}\text{H}_{24}\text{ClCuN}_3\text{O}_6$	$[\text{Cu}^{\text{II}}\text{L}^{\text{H}3}](\text{ClO}_4)$ $\text{C}_{19}\text{H}_{24}\text{ClCuN}_3\text{O}_6$	$[\text{Cu}^{\text{II}}\text{L}^{\text{OMe}3}](\text{ClO}_4)$ $\text{C}_{44}\text{H}_{62}\text{Cl}_2\text{Cu}_2\text{N}_6\text{O}_{15}$	$[\text{Cu}^{\text{II}}\text{L}^{\text{H}4}](\text{ClO}_4)$ $\text{C}_{18}\text{H}_{22}\text{ClCuN}_3\text{O}_6$	$[\text{Cu}^{\text{II}}\text{L}^{\text{H}5}]_2(\text{ClO}_4)_2$ $\text{C}_{38}\text{H}_{48}\text{Cl}_2\text{Cu}_2\text{N}_6\text{O}_{12}$
molecular weight ($\text{g}\cdot\text{mol}^{-1}$)	525.43	488.39	1112.98	475.38	978.80
T (K)	100(2)	296	100(2)	89(2)	100(2)
crystal system	Monoclinic	Monoclinic	Triclinic	Monoclinic	Orthorhombic
space group	$P2_1/c$	$C2/c$	P-1	$I2/a$	Pbca
Z	4	8	4	8	4
a (Å)	13.1270(2)	11.5021 (3)	13.9094(3)	19.0697(4)	12.2844(2)
b (Å)	13.7157(2)	18.7307 (5)	18.2391(4)	10.6833(2)	14.1806(2)
c (Å)	12.1763(2)	20.7277 (7)	20.6775(6)	18.9974(3)	23.1490(3)
α (°)	90	90	90.039(2)	90	90
β (°)	103.203(2)	95.504 (1)	91.901(2)	95.766(2)	90
γ (°)	90	90	111.884(2)	90	90
V (Å ³)	2134.34(6)	4445.0 (2)	4864.6(2)	3850.71(12)	4032.56(10)
density ($\text{g}\cdot\text{cm}^{-3}$)	1.635	1.460	1.520	1.640	1.612
R ₁	0.0308	0.045	0.1565	0.0382	0.0878
wR ₂	0.0809	0.138	0.3908	0.1218	0.2657

5

Crystal structure of $[\text{Cu}^{\text{II}}\text{L}^{\text{H}5}]_2(\text{ClO}_4)_2$

Green single crystals of $[\text{Cu}^{\text{II}}\text{L}^{\text{H}5}]_2(\text{ClO}_4)_2$ were obtained by slow diffusion of diethyl ether into a solution of the complex dissolved in a mixture of CH_3CN and CH_3OH , and crystallises in the orthorhombic crystal system and Pbca space group. The molecular structure and selected bond lengths and bond angles relating to the coordination environment of the metal and also bond lengths related to similar compounds are given in Figure 3 and Table 2 respectively. The structure is a dinuclear, comprising two similar Cu(II) centers. Each copper atom has a pentacoordinate square-pyramidal geometry. N(1), N(2), N(3) and O(2) of a deprotonated Schiff base bind four coordination sites of Cu(1). Similarly, Cu(2) is coordinated by N(1), N(2),

N(3) and O(2) of another deprotonated Schiff base. The fifth, apical, coordination site of each Cu(1) is occupied by O(2) from another ligand, thereby forming a di-phenoxy-bridged dimer, while the hydroxypropyl arm (O(1)) of the ligand remains uncoordinated (Figure 3). The charge distribution was assigned based on the presence of only two ClO_4^- anions which make the complex a dication with two deprotonated ligands $\text{L}^{\text{H}5}$. Each phenoxy oxygen atom is bridging two complexes in an antisymmetric fashion giving Cu–O_{phenoxy} bond lengths of 2.407 and 1.937 Å - which is in the range of previously reported structures for copper(II) dimeric complex having phenoxy bridge.^{36–38} The coordination geometry around the copper centers is best described by the use of the τ -criterion,³⁷ indicating that the coordination geometry in $[\text{Cu}^{\text{II}}\text{L}^{\text{H}5}]_2^+$ is only slightly from square-

pyramidal distorted ($\tau = 0.11$). In this compound, N(1), N(2), N(3) and O(2) related to the same ligand occupy the equatorial positions and O(2)', from the second ligand, occupies the apical position. The τ value for both Cu(1) in $[\text{Cu}^{\text{II}}\text{L}^{\text{H5}}]_2(\text{ClO}_4)_2$ is 0.11, which is similar to the value of Cu(II) in the monomers. Thus the geometries of both the copper centers in $[\text{Cu}^{\text{II}}\text{L}^{\text{H5}}]_2(\text{ClO}_4)_2$ are distorted square pyramidal. A 5,6,6-chelate ring sequence is observed in the dimer $[\text{Cu}^{\text{II}}\text{L}^{\text{H5}}]_2^+$, with the expected square-pyramidal coordination geometry for both Cu(II).

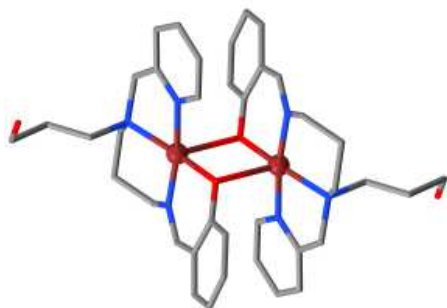


Figure 3. Perspective view of $[\text{Cu}^{\text{II}}\text{L}^{\text{H5}}]_2(\text{ClO}_4)_2$. Hydrogen atoms and anions are omitted for clarity. Cu, C, N and O are represented in dark red, gray, blue and red, respectively.

In contrast with the coordinated ligand L^{naphH2} , L^{H3} , L^{OMe3} and L^{H4} in $[\text{Cu}^{\text{II}}\text{L}^{\text{naphH2}}](\text{ClO}_4)$, $[\text{Cu}^{\text{II}}\text{L}^{\text{H3}}](\text{ClO}_4)$, $[\text{Cu}^{\text{II}}\text{L}^{\text{OMe3}}](\text{ClO}_4)$ and $[\text{Cu}^{\text{II}}\text{L}^{\text{H4}}](\text{ClO}_4)$ complexes, respectively, the ligand anion in complex $[\text{Cu}^{\text{II}}\text{L}^{\text{H5}}]_2^+$ uses only four of the five donor groups binding to the copper atom, in which the hydroxypropyl arm remains uncoordinated and the phenolic oxygen atom bridges two Cu(II) atoms resulting in a Cu_2O_2 ring. This is not exclusively due to the steric situation in $[\text{Cu}^{\text{II}}\text{L}^{\text{H5}}]_2(\text{ClO}_4)_2$, but to the low stability of the six-membered chelate ring which would have been formed with the hydroxypropyl ligand arm: a similar behavior of related aliphatic tripodal ligands¹⁰ and also asymmetric tripodal ligand with two aliphatic and one aromatic arms has been already reported.²⁶ In addition, the stability of the copper complex with the ligand **trpn**, which exclusively forms six-membered chelate rings, is shown to be about 10^5 times lower than the stability of the corresponding **tren** complex that contains only five-membered chelate rings.^{9c} Examination of the Cu(II) complexes in the present study and the literature shows that Cu(II) atom in tripodal complexes have a great flexibility in adoption of the number of the chelate rings sequence around the metal atom to form a square pyramidal geometry around the central ion as observed for ($[\text{Cu}^{\text{II}}\text{L}^{\text{naphH2}}](\text{ClO}_4)$, 5,5,6,6, $\tau = 0.10$; $[\text{Cu}^{\text{II}}\text{L}^{\text{H3}}](\text{ClO}_4)$, 5,5,7,6, $\tau = 0.11$; $[\text{Cu}^{\text{II}}\text{L}^{\text{OMe3}}](\text{ClO}_4)$, 5,5,7,6, $\tau = 0.066$; $[\text{Cu}^{\text{II}}\text{L}^{\text{H4}}](\text{ClO}_4)$, 5,6,5,6, $\tau = 0.39$) and ($[\text{Cu}^{\text{II}}\text{L}^{\text{H5}}]_2(\text{ClO}_4)_2$, 5,6,6, $\tau = 0.11$), but it should be noted that Cu(II) in these types of complexes are not stable against the high number of six-membered chelate rings around the metal.^{9c} For the dinuclear complex $[\text{Cu}^{\text{II}}\text{L}^{\text{H5}}]_2(\text{ClO}_4)_2$ the hypothetical mononuclear $[\text{Cu}^{\text{II}}\text{L}^{\text{H5}}](\text{ClO}_4)$ would possess a 5,6,6,6 chelate ring sequence around the Cu(II) atom which, due to the high number of six-membered chelate rings, would be unstable. In order to form the stable structure with square pyramidal geometry, the hypothetical

mononuclear complex would prefer to form a dinuclear structure with a 5,6,6 chelate ring sequence with a second identical ligand. Table 3 show the comparison of the structural parameter (τ -value) for Cu(II) complexes characterized here.

Theoretical studies

As described above, the present study brought us three interesting results. Firstly, the formation of mononuclear five-coordinate complexes, with a majority of ligands, and dinuclear complexes, with the remaining ligands. Secondly, X-ray crystal structures showed that hydrogen bonding can exist between two mononuclear five-coordinate complexes. Thirdly, mass spectra of both mononuclear and dinuclear complexes always show two characteristic peaks, one corresponding to a mononuclear fragment and one corresponding to a dinuclear fragment. In order to understand these results theoretical calculations were undertaken. The strength of interaction between two mononuclear four-coordinated fragments in one dinuclear complex and hydrogen bonding between two mononuclear five-coordinated complexes were evaluated (see Figure 4). From this study it is clear that one of the coordinated arms in the mononuclear complex leaves the metal ion and then the resulting four-coordinated complex can be dimerized. As can be seen in Figures 3 and 4(a) in these dinuclear complexes, the hydroxyl group of the hydroxypropyl arm is not coordinated to the metal ion. Thus the strength of the interaction between hydroxyl group and metal ion was evaluated, to figure out why it leaves the metal ion. However, the value of interaction energy between the metal ion and whole ligand in these complexes was calculated first. As can be seen in Table 4, the values of interaction energies are relatively large and are in the range 629-634 kcal/mol. Thus in all mononuclear complexes the Schiff base ligands are tightly bonded to the central metal ion. However, the data show that the interaction energy between two mononuclear fragments in the dinuclear complex $[\text{Cu}^{\text{II}}\text{L}^{\text{H5}}]_2(\text{ClO}_4)_2$ is very small and only -4.24 kcal/mol (see Table 5). Such a small interaction energy is not surprising as the interacting fragments are both cations. This explains why even in the mass spectra of the dinuclear complexes the major peak corresponds to a mononuclear complex. Indeed, inside the mass spectrometer the dinuclear complex readily breaks into two mononuclear complexes. Two forms, **I** and **II**, were considered for one of the mononuclear fragments of the dinuclear complex $[\text{Cu}^{\text{II}}\text{L}^{\text{H5}}]_2(\text{ClO}_4)_2$ and the geometry optimised for both them (see Figure 5e and 5f). The difference between the above forms is that in form **I** the hydroxyl group is not coordinated to the metal ion but is indeed coordinated in form **II**. The data showed that the energy difference between two above forms is only -2.57 kcal/mol. Thus the interaction between the hydroxyl group and the central metal ion seems to be very weak. This means that the hydroxyl group simply leaves the metal ion, resulting in four-coordinated copper complexes which can be dimerized. This is the reason why in mass spectra of all complexes there is a very small peak corresponding to a dinuclear complex.

Cite this: DOI: 10.1039/c0xx00000x

FULL PAPER

www.rsc.org/xxxxxx

Table 2. Comparison of selected bond lengths [Å] and angles [°] for [Cu^{II}L^{naph2}](ClO₄), [Cu^{II}L^{H3}](ClO₄), [Cu^{II}L^{OMe3}](ClO₄), [Cu^{II}L^{H4}](ClO₄) and [Cu^{II}L^{H5}]₂(ClO₄)₂ complexes.

	[Cu ^{II} L ^{naph2}](ClO ₄)	[Cu ^{II} L ^{H3}](ClO ₄)	[Cu ^{II} L ^{OMe3}](ClO ₄)	[Cu ^{II} L ^{H4}](ClO ₄)	[Cu ^{II} L ^{H5}] ₂ (ClO ₄) ₂	Sq pyr Cu(II) in the literature	References
Bond length [Å]							
M(1)-N _(imine)	1.9486(15)	1.989 (3)	2.008(10)	1.929(2)	1.969(7)	1.923-1.969	14, 31
M(1)-N _(py)	2.0122(16)	2.025 (3)	2.014(11)	1.979(2)	2.006(7)	1.925-2.006	31, 32
M(1)-N _(amine)	2.0910(15)	2.125 (2)	2.148(9)	2.062(2)	2.057(7)	1.979-2.062	19, 32-34
M(1)-O _(phenolic)	1.9234(12)	1.921 (2)	1.927(8)	1.9172(17)	1.937(5)	1.917-2.096	19, 31, 35-38
M(1)...O _(hydroxyalkyl)	2.3802(13)	2.241 (2)	2.222(9)	2.2195(18)	5.415	1.916-2.339	19
M(1)-O _(2#1)					2.407(6)	2.423	38
M(1)...M(1)					3.240	2.2729-3.001	19, 31
Bond angle [°]							
O _(phenolic) -M(1)-N _(imine)	91.89(6)	90.19 (9)	91.0(4)	95.54(8)	92.6(3)		
O _(phenolic) -M(1)-N _(py)	90.98(6)	88.29(10)	86.4(4)	94.89(8)	90.5(3)		
N _(imine) -M(1)-N _(py)	164.51(6)	159.96 (11)	160.0(4)	155.64(9)	172.0(3)		
O _(phenolic) -M(1)-N _(amine)	170.51(6)	166.57 (10)	164.0(4)	179.08(8)	165.4(3)		
N _(imine) -M(1)-N _(amine)	96.21(6)	102.86(11)	104.0(4)	86.37(9)	94.2(3)		
N _(py) -M(1)-N _(amine)	82.53(6)	80.54(11)	81.3(4)	84.27(8)	81.2(3)		
O _(phenolic) -M(1)-O _(hydroxyalkyl)	91.77(5)	94.75 (9)	94.3(3)	90.62(7)			
N _(imine) -M(1)-O _(hydroxyalkyl)	109.15(5)	99.15(10)	97.1(4)	95.53(8)			
N _(py) -M(1)-O _(hydroxyalkyl)	85.96(5)	100.92(10)	102.9(4)	106.77(8)			
N _(amine) -M(1)-O _(hydroxyalkyl)	80.92(5)	80.2(9)	78.6(3)	89.27(7)			
O _(phenolic) -M(1)-O _(2#1)					84.2(2)		
N _(imine) -M(1)-O _(2#1)					91.0(2)		
N _(py) -M(1)-O _(2#1)					96.7(2)		
N _(amine) -M(1)-O _(2#1)					108.6(2)		

Table 3. Comparison of τ-value in 5-coordinated Cu complexes.

5-coordinated Complexes	chelate ring sequence	τ-value
[Cu ^{II} L ^{naph2}](ClO ₄)	5,5,6,6	0.10
[Cu ^{II} L ^{H3}](ClO ₄)	5,5,7,6	0.11
[Cu ^{II} L ^{OMe3}](ClO ₄)	5,5,7,6	0.066
[Cu ^{II} L ^{H4}](ClO ₄)	5,6,5,6	0.39
[Cu ^{II} L ^{H5}] ₂ (ClO ₄) ₂	5,6,6	0.11

Among the complexes synthesized here, both [Cu^{II}L^{H5}]₂(ClO₄)₂ and [Cu^{II}L^{H4}](ClO₄) complexes have the hydroxyl group at the end of a propyl chain. For all the other complexes the hydroxyl group is at the end of an ethyl chain. Indeed, only in the case of [Cu^{II}L^{H5}]₂(ClO₄)₂ and [Cu^{II}L^{H4}](ClO₄) do we observe an unstable six-membered chelate ring forming upon coordination of the hydroxyl group. For all other complexes the coordination of the hydroxyl group leads to formation of a more stable five-membered chelate ring. Thus it seems that the formation of a dinuclear complex in which the hydroxyl group remained uncoordinated is quite expectable for both [Cu^{II}L^{H5}]₂(ClO₄)₂ and [Cu^{II}L^{H4}](ClO₄) complexes. However X-ray crystal structure

analysis confirmed the formation of a dinuclear complex only in the case of the former complex. Thus two forms **I** and **II** for [Cu^{II}L^{H4}](ClO₄) were also considered and optimized (see Figure 5c and 5d). As can be seen in Table 6, the data show that the energy difference between the above forms is about -5.32 kcal/mol. Thus it seems that the interaction energy between the hydroxyl group and metal ion in complex [Cu^{II}L^{H4}](ClO₄) is relatively larger than that in complex [Cu^{II}L^{H5}]₂(ClO₄)₂. On the other hand, the interaction energy between two mononuclear fragments in the dinuclear complex [Cu^{II}L^{H5}]₂(ClO₄)₂ was only -4.24 kcal/mol. The above interaction is larger than -2.57 kcal/mol and less than -5.3 kcal/mol, calculated energy difference between forms **I** and **II** in complexes [Cu^{II}L^{H5}]₂(ClO₄)₂ and [Cu^{II}L^{H4}](ClO₄), respectively. This explains why the complex [Cu^{II}L^{H5}]₂(ClO₄)₂ is dimerized while [Cu^{II}L^{H4}](ClO₄) remained mononuclear. For [Cu^{II}L^{H5}]₂(ClO₄)₂, in contrast to [Cu^{II}L^{H4}](ClO₄), the value of interaction energy between two four coordinated fragments is larger than that between the hydroxyl group and central metal ion.

Cite this: DOI: 10.1039/c0xx00000x

FULL PAPER

www.rsc.org/xxxxxx

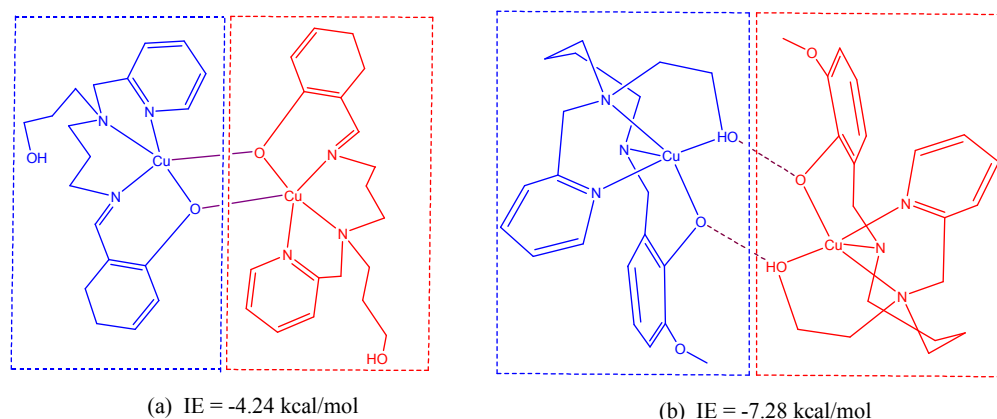


Figure 4. Interacted four-coordinated fragments in dinuclear complex $[\text{Cu}^{\text{II}}\text{L}^{\text{H5}}]_2(\text{ClO}_4)_2$ (a) and hydrogen bonding between two $[\text{Cu}^{\text{II}}\text{L}^{\text{OMe3}}](\text{ClO}_4)$ complexes (b).

Table 4. Calculated interaction energies(IE) between the metal ion and pentadentate ligands synthesized here.

Compound	E_{el} (Hartree)			IE (kcal/mol)
	Cu^{2+}	$\text{L}^{\text{ald-*}}$	$[\text{CuL}^{\text{ald}}]^+$	
$[\text{Cu}^{\text{II}}\text{L}^{\text{OMe3}}](\text{ClO}_4)$	-1639.151635	-1165.9898167	-2806.1509036	-633.44
$[\text{Cu}^{\text{II}}\text{L}^{\text{H3}}](\text{ClO}_4)$	-1639.151635	-1051.6149949	-2691.7726555	-631.29
$[\text{Cu}^{\text{II}}\text{L}^{\text{naphH2}}](\text{ClO}_4)$	-1639.151635	-1165.7856412	-2805.939729	-629.05
$[\text{Cu}^{\text{II}}\text{L}^{\text{H4}}](\text{ClO}_4)$	-1639.151635	-1012.3607015	-2652.5239637	-634.81

* Frozen in the optimized geometry of the $[\text{CuL}^{\text{ald}}]^+$ complex.

5

In addition, we believe that the formation of hydrogen bonding between two mononuclear five-coordinated complexes prevents the formation of a dinuclear complex between two four-coordinated fragments. As seen in the previous section the X-ray crystal structure of the complex $[\text{Cu}^{\text{II}}\text{L}^{\text{OMe3}}](\text{ClO}_4)$ showed that the hydrogen bonding is formed between two mononuclear complexes. Indeed the coordination of the hydroxyl group to the metal ion and then the formation of hydrogen bond between two molecules of such five-coordinated complex in $[\text{Cu}^{\text{II}}\text{L}^{\text{OMe3}}](\text{ClO}_4)$ prevent the formation of a dinuclear complex which is formed in the case of $[\text{Cu}^{\text{II}}\text{L}^{\text{H5}}]_2(\text{ClO}_4)_2$. the value of the interaction between two mononuclear $[\text{Cu}^{\text{II}}\text{L}^{\text{OMe3}}](\text{ClO}_4)$ complexes due to hydrogen

bonding is about -7.28 kcal/mol (see Fig 4). Interestingly, the latter value is larger than -4.24 kcal/mol, the interaction between two fragments in dinuclear complex $[\text{Cu}^{\text{II}}\text{L}^{\text{H5}}]_2(\text{ClO}_4)_2$, and larger than -2.57 and -5.3 kcal/mol, the energy difference between forms I and II of complexes $[\text{Cu}^{\text{II}}\text{L}^{\text{H5}}]_2(\text{ClO}_4)_2$ and $[\text{Cu}^{\text{II}}\text{L}^{\text{H4}}](\text{ClO}_4)$, respectively. Therefore these complexes are special cases in which the intermolecular interactions (herein hydrogen bonding) between two complexes can be stronger than some weak intramolecular metal-donor atom interactions. The formation of a mononuclear complex or a dinuclear one thus depends on relative strength of inter- and intramolecular interactions.

Table 5. Calculated interaction energy (IE) between two $[\text{Cu}^{\text{II}}\text{L}^{\text{OMe3}}](\text{ClO}_4)$ complexes bonded through hydrogen bonding and also two mononuclear fragments in dinuclear $[\text{Cu}^{\text{II}}\text{L}^{\text{H5}}]_2(\text{ClO}_4)_2$

Compound	E_{el} (Hartree)			IE (kcal/mol)
	First complex/fragment*	Second complex/fragment*	Whole compound	
$[\text{Cu}^{\text{II}}\text{L}^{\text{OMe3}}](\text{ClO}_4)$	-2806.1480886	-2806.1477506	-5612.3074422	-7.28
$[\text{Cu}^{\text{II}}\text{L}^{\text{H5}}]_2(\text{ClO}_4)_2$	-2691.7619224	-2691.7619224	-5383.5306096	-4.24

* Frozen in the optimized geometry of whole compound

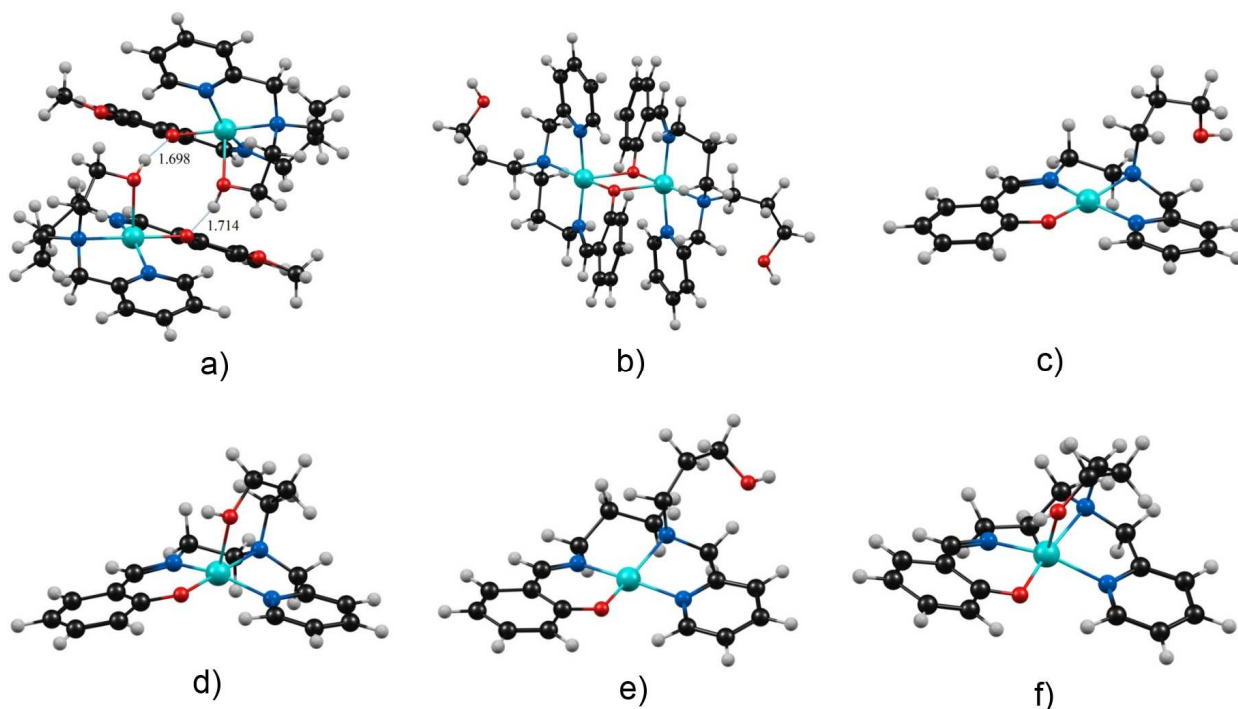


Figure 5. The optimized structures for complexes/fragments studied here. a) two $[\text{Cu}^{\text{II}}\text{L}^{\text{OMe}3}](\text{ClO}_4)$ complexes bounded through hydrogen bonding. b) dinuclear $[\text{Cu}^{\text{II}}\text{L}^{\text{H}5}]_2(\text{ClO}_4)_2$ complex. c) form I of $[\text{Cu}^{\text{II}}\text{L}^{\text{H}4}](\text{ClO}_4)$. d) form II of $[\text{Cu}^{\text{II}}\text{L}^{\text{H}4}](\text{ClO}_4)$. e) form I of one fragments in $[\text{Cu}^{\text{II}}\text{L}^{\text{H}5}]_2(\text{ClO}_4)_2$. f) form II of one fragments in $[\text{Cu}^{\text{II}}\text{L}^{\text{H}5}]_2(\text{ClO}_4)_2$.

Table 6. Calculated energy difference (ΔE) between the optimized structures of forms I and II considered here for mononuclear $[\text{Cu}^{\text{II}}\text{L}^{\text{H}4}](\text{ClO}_4)$ and one mononuclear fragment in dinuclear $[\text{Cu}^{\text{II}}\text{L}^{\text{H}5}]_2(\text{ClO}_4)_2$.

Compound	E_{el} (Hartree)		ΔE (kcal/mol)
	Form I	Form II	
$[\text{Cu}^{\text{II}}\text{L}^{\text{H}4}](\text{ClO}_4)$	-	-	-5.32
	2691.7690481	2691.7731458	
$[\text{Cu}^{\text{II}}\text{L}^{\text{H}5}]_2(\text{ClO}_4)_2$	-	-	-2.57
	2652.5239637	2652.5154793	

10 Conclusion

In summary, we have reported the successful synthesis of 14 new mononuclear and a few dinuclear Cu(II) complexes by condensation of amines (3-6) with related aldehydes in the presence of Cu(II) metal ion. X-ray crystal structure determinations of $[\text{Cu}^{\text{II}}\text{L}^{\text{naphht}2}](\text{ClO}_4)$, $[\text{Cu}^{\text{II}}\text{L}^{\text{H}3}](\text{ClO}_4)$, $[\text{Cu}^{\text{II}}\text{L}^{\text{OMe}3}](\text{ClO}_4)$ and $[\text{Cu}^{\text{II}}\text{L}^{\text{H}4}](\text{ClO}_4)$ revealed them to be monomeric, except for the dimeric $[\text{Cu}^{\text{II}}\text{L}^{\text{H}5}]_2(\text{ClO}_4)_2$. There is a distorted square pyramidal environment around the central ion in both mononuclear and dinuclear complexes. In this work, emphasis has been put on the examination of structural relationships in the complexation behavior. By comparing crystal structures of the complexes identified to date, all of them use four donor groups of the ligand (three nitrogen atom and phenoxy oxygen atom) to bind the metal atom and the

differences observed is related to hydroxyalkyl arms. These arms are not coordinated to the metal ion in all complexes but in both coordinated and non-coordinated state they remain protonated. Examination of X-ray crystal structures of Cu(II) complexes in the present study show that in the Cu(II) complexes with an ethyl-amino arm, the hydroxypropyl group is bound to the Cu(II) atom, while in the Cu(II) complexes with a propyl-amino arm, the hydroxypropyl arm remains uncoordinated and a dinuclear Cu(II) complex is formed. According to theoretical study, the interaction between the hydroxyl group and the central metal ion seems to be very weak thus the hydroxyl group can leave the metal ion, yielding four-coordinated Cu(II) complexes which can be dimerized. The theoretical study also showed that the formation of a mononuclear complex or a dinuclear one depends on relative strength of inter- and intramolecular interactions. In Cu(II) complexes with an hydroxyethyl arm, there is a stronger interaction between the hydroxyl group and the central metal ion due to the formation of a stable five-membered chelate ring upon the coordination of the hydroxyl group to metal ion. In the case of the Cu(II) complexes with hydroxypropyl arm, an unstable six-membered chelate ring forms upon the coordination of the hydroxyl group - the formation of dinuclear structures is more expectable in this case. Note that both ligands $\text{L}^{\text{H}5}$ and $\text{L}^{\text{H}4}$ have a hydroxypropyl arm, but the X-ray crystal structure analysis confirmed the formation of a dinuclear copper complex only in the case of $\text{L}^{\text{H}5}$. By comparison of the structures, it seems that both aliphatic

linkages are effective on the structure of dimeric complexes. According to theoretical studies, the value of interaction energy between two four coordinate fragments in dinuclear $[\text{Cu}^{\text{II}}\text{L}^{\text{H5}}]_2(\text{ClO}_4)_2$ complex, in contrast to $[\text{Cu}^{\text{II}}\text{L}^{\text{H4}}](\text{ClO}_4)$, is larger than that between the hydroxyl group and the central metal ion. Thus we can assume that a mononuclear five coordinated complex forms first, and in a second time the hydroxyl group leaves the metal ion, resulting in a four-coordinated complex which can be dimerized. In addition of intramolecular interactions, intermolecular interactions are also important in the formation of a mononuclear complex or a dinuclear one. The theoretical study also supported our assumption that the formation of hydrogen bonds between two mononuclear five-coordinated complexes prevents the formation of a dinuclear complex between two four coordinate fragments.

Experimental

General remarks

Pyridine 2-carbaldehyde, 2-Hydroxy-3-methoxybenzaldehyde, 2-hydroxybenzaldehyde, 2-hydroxy-1-naphthaldehyde and metal salt were obtained from Aldrich and used without further purification. 3,5-Di-tert-butyl-2-hydroxybenzaldehyde was synthesised according to the literature procedure.⁴² All other chemicals and solvents were of reagent grade and were used as received except for methanol that was dried (Mg) before use.

Caution!

Whilst no problems were encountered in the course of this work, perchlorate mixtures are potentially explosive and should therefore be handled with appropriate care.

Infrared spectra were obtained between 4000 and 400 cm^{-1} on a Bruker Alpha FT-ATR IR spectrometer with a diamond anvil Alpha-P module for all complexese. UV-vis spectra were recorded on a Jasco V550 spectrophotometer. ESI mass spectra were recorded at the University of Otago on a Bruker MicroTOFQ spectrometer exception for $[\text{Cu}^{\text{II}}\text{L}^{\text{H3}}](\text{ClO}_4)$, $[\text{Cu}^{\text{II}}\text{L}^{\text{OMe3}}](\text{ClO}_4)$ and $[\text{Cu}^{\text{II}}\text{L}^{\text{tBu3}}](\text{ClO}_4)$ complexes that the spectra were recorded using a Kratos-MS- 50T spectrometer. Room temperature magnetic moments were determined using a Johnson Matthey MSB-MK1 magnetic susceptibility balance. Standard microanalysis for all complexes were carried out by a Perkin-Elmer, CHNS/O elemental analyzer model 2400. ^1H and ^{13}C NMR spectra were taken in CDCl_3 on a Jeol 90 MHz spectrometer using $\text{Si}(\text{CH}_3)_4$ as an internal standard. Crystals suitable for X-ray diffraction were obtained by slow diffusion of diethyl ether vapor into methanol or a mixture of methanol and acetonitrile. Single crystal X-ray crystallographic data were collected at 100 K for $[\text{Cu}^{\text{II}}\text{L}^{\text{naphH2}}](\text{ClO}_4)$, $[\text{Cu}^{\text{II}}\text{L}^{\text{OMe3}}](\text{ClO}_4)$ and $[\text{Cu}^{\text{II}}\text{L}^{\text{H5}}]_2(\text{ClO}_4)_2$ ($\lambda = 1.54184$) and also at 89 K for

$[\text{Cu}^{\text{II}}\text{L}^{\text{H4}}](\text{ClO}_4)$ ($\lambda = 0.71073$) on a Bruker Kappa APEX II area detector diffractometer (University of Otago), using graphite monochromatic Mo-K α radiation. In the case of $[\text{Cu}^{\text{II}}\text{L}^{\text{H3}}](\text{ClO}_4)$ complex, single crystal X-ray crystallographic data was collected at 296 K ($\lambda = 1.54184$) on Bruker SMART BREEZE CCD diffractometer with APEX2 software.⁴³ The data were collected for Lorentz and polarization effects and semi-empirical absorption corrections (SCALE) were applied. The structures were solved by direct or Patterson methods (SHELXS-97)⁴⁴ and refined against all F^2 data (SHELX-97).⁴⁵ All non-hydrogen atoms were modelled anisotropically except where noted. Unless otherwise specified, hydrogen atoms were inserted at calculated positions and rode on the atoms to which they were attached. In the case of this complex, absorption correction applied to collected data by multi scan, SADAPS V2012/1 software.⁴³ The title compound solved by direct methods⁴⁶ using SHELXS-97 and refined with SHELXL-97.⁴⁶ The weighted R-factor, wR and goodness of fit S are based on F^2 . The threshold expression of $F^2 > 2\sigma(F^2)$ is used only for calculating R-factors. All estimated standard deviations (e.s.d's) are estimated using the full covariance matrix. The cell e.s.d's are taken into account individually in the estimation of e.s.d.'s in distances, angles, and torsion angles; correlations between e.s.d.'s in cell parameters are only used when they are defined by crystal symmetry. All non-hydrogen atoms were refined anisotropically and hydrogen atoms were added according to the theoretical model. In the case of complex $[\text{Cu}^{\text{II}}\text{L}^{\text{OMe3}}](\text{ClO}_4)$, we were not able to refine the X-ray crystal structure of this complex exactly.

Computational details

The crystallographic structure of all $[\text{CuL}^{\text{ald}}]^+$ complexes were fully optimized with def2-SVP basis set at M06⁴⁷ level of theory. The calculated bond lengths and bond angles in optimized complexes were in good agreement with corresponding experimental data. Calculated root mean squares (RMS) for metal-ligand bond distances were less than 0.055 (see Table 7). The interaction energy between the Cu^{2+} metal ion and the anionic ligand in mononuclear complexes was calculated with the following equation:

$\Delta E = E_{\text{AB}} - (E_{\text{A}}^{\text{AB}} + E_{\text{B}}^{\text{AB}})$, where E_{AB} is the minimized energy of the $[\text{CuL}^{\text{ald}}]^+$ complexes and E_{A}^{AB} and E_{B}^{AB} are the energies of Cu^{2+} and L^- fragments, respectively, frozen in the geometry of this structure. Also interaction energies between the two mononuclear four coordinate fragments in one dinuclear $[\text{Cu}^{\text{II}}\text{L}^{\text{H5}}]_2(\text{ClO}_4)_2$ complex and two five coordinate $[\text{Cu}^{\text{II}}\text{L}^{\text{OMe3}}](\text{ClO}_4)$ complexes bonded through hydrogen bonding were calculated with same formul, where the E_{AB} is the minimized energy of the whole compound and E_{A}^{AB} and E_{B}^{AB} are the energies of the considered fragments. All calculations were performed using the Gaussian09 program.⁴⁸

Cite this: DOI: 10.1039/c0xx00000x

FULL PAPER

www.rsc.org/xxxxxx

Table 7. Computed and experimental Cu-N and Cu-O bond lengths (Å) for [CuL^{ald}]⁺ complexes*

Compounds	Cu-N _{amine}	Cu-N _{py}	Cu-N _{imine}	Cu-O [•]	Cu-OH	RMS
[Cu ^{II} L ^{OMe3}](ClO ₄)	2.190 <i>2.136</i>	2.045 <i>2.039</i>	2.009 <i>2.013</i>	1.944 <i>2.013</i>	2.209 <i>2.232</i>	0.041
[Cu ^{II} L ^{H3}](ClO ₄)	2.227 <i>2.125</i>	2.046 <i>2.025</i>	1.985 <i>1.990</i>	1.916 <i>1.921</i>	2.298 <i>2.236</i>	0.054
[Cu ^{II} L ^{naph2}](ClO ₄)	2.140 <i>2.091</i>	2.030 <i>2.012</i>	1.940 <i>1.949</i>	1.916 <i>1.923</i>	2.339 <i>2.380</i>	0.030
[Cu ^{II} L ^{H4}](ClO ₄)	2.113 <i>2.062</i>	2.017 <i>1.979</i>	1.935 <i>1.928</i>	1.905 <i>1.917</i>	2.250 <i>2.220</i>	0.032
[Cu ^{II} L ^{H5}] ₂ (ClO ₄) ₂	2.102 <i>2.056</i>	2.027 <i>2.006</i>	1.988 <i>1.970</i>	1.975 <i>1.938</i>	2.340** <i>2.407</i>	0.042

* The data obtained at the M06/def2-SVP level are given as plain text and experimental data are in italic.

** For this complex this is the distance between Cu(1)–O(2) bond.

Synthesis and Characterization

General synthesis of unsymmetrical tripodal amines (3-6)

2-Aminoethanol (1.22 g, 20 mmol) or 3-Aminopropan-1-ol (1.50 g, 20 mmol) in dry EtOH (100 mL) was added dropwise to a solution of pyridine-2-carbaldehyde (2.14 g, 20 mmol) in dry EtOH (100 mL) over a period of 2 h separately. The mixture was refluxed under stirring for 12 h. Solid sodium borohydride (3.02 g, 80 mmol) was then added slowly and the reaction mixture was stirred for a further 12 h before it was filtered. The filtrate was reduced to 20 mL by rotary evaporation. Water (50 mL) was added and the products extracted with chloroform (3 x 50 mL). The combined extracts were dried over magnesium sulfate, filtered, then taken to dryness by rotary evaporation. The resulting brown oil (1.52 g, 10 mmol (starting with 2-Aminoethano, **1'**) or 1.66 g, 10 mmol (starting with 3-Aminopropan-1-ol, **2'**), 77–86%) was dissolved in acetonitrile (70 mL), solid K₂CO₃ (2.07 g, 15 mmol) added, and the mixture brought to reflux before a solution of N-(4-bromobutyl)phthalimide (2.81 g, 10 mmol) was added dropwise to **1'**, or N-(2-bromoethyl)phthalimide (2.53 g, 10 mmol) or N-(3-bromopropyl)phthalimide (2.67 g, 10 mmol) or N-(4-bromobutyl)phthalimide (2.81 g, 10 mmol) in acetonitrile (70 mL) to **2'**. The mixture was refluxed for 48 h and then filtered hot. The filtrate was reduced to dryness by rotary evaporation. The brown oil residue was boiled under reflux for 12 h in aqueous HCl (25%, 100 mL) then evaporated to a small volume (ca. 25 mL) under vacuum and cooled in a refrigerator for several hours. The resulting solid was filtered off and discarded, and the filtrate evaporated to dryness under vacuum. Water (50 mL) was added to the resulting brown residue and the pH adjusted to 12 with sodium hydroxide before extracting

with chloroform (3 x 50 mL). The combined extract was dried over magnesium sulfate, filtered and the chloroform removed from the filtrate by rotary evaporation to leave the products, **3-6**, as brown oils.

Synthesis of 2-((4-aminobutyl)(pyridin-2-ylmethyl)amino)ethanol (3)

Yield: 1.34 g (60%). Anal. Calc. for C₁₂H₂₁N₃O (MW: 223.17): C, 64.54; H, 9.48; N, 18.82. Found: 64.35; H, 9.25; N, 19.10%. IR (Nujolmull, cm⁻¹) 3354, 3272 ν (NH₂), 1591 ν (C=N)_{py}. ¹H NMR (CDCl₃, ppm) δ = 1.36–1.55 (m, 4H); 2.33 (b, 3H), 2.55–2.72 (m, 6H); 3.58–3.60 (t, 2H); 3.78 (s, 2H); 7.14–7.17 (m, 1H); 7.14–7.17 (t, 1H); 7.29 (d, 1H); 7.62–7.66 (td, 1H); 8.52 (d, 1H). ¹³C NMR (CDCl₃, ppm) δ = 24.057; 29.248; 40.432; 54.065; 56.110; 58.750; 59.688; 121.349; 122.493; 135.879; 148.314; 159.228.

Synthesis of 3-((2-aminoethyl)(pyridin-2-ylmethyl)amino)propan-1-ol (4)

Yield: 1.61 g (77%). Anal. Calc. for C₁₁H₁₉N₃O (MW: 209.15): C, 63.13; H, 9.15; N, 20.08. Found: 64.05; H, 9.25; N, 19.70%. IR (Nujol mull, cm⁻¹) 3341, 3262 ν (NH₂), 1593 ν (C=N)_{py}. ¹H NMR (CDCl₃, ppm) δ = 1.309–1.625 (m, 2H); 2.432–2.631 (m, 6H); 3.334–3.640 (m, 4H); 4.466 (s, 3H); 6.837–7.403 (m, 3H); 8.234 (d, 1H). ¹³C NMR (CDCl₃, ppm) δ = 29.061; 38.186; 51.476; 54.671; 59.340; 59.826; 121.420; 122.367; 135.981; 148.220; 158.791.

Synthesis of 3-((3-aminopropyl)(pyridin-2-ylmethyl)amino)propan-1-ol (5)

Yield: 1.92 g (86%). Anal. Calc. for C₁₂H₂₁N₃O (MW: 223.31): C, 64.54; H, 9.48; N, 18.82. Found: 64.20; H, 9.65; N, 18.90%. IR (Nujol mull, cm⁻¹) 3352, 3271 ν (NH₂), 1591 ν (C=N)_{py}. ¹H NMR (CDCl₃, ppm) δ = 1.497 (m, 4H); 2.309–2.546 (m, 6H); 3.482 (s, 4H); 4.436 (s, 3H); 6.856–7.505 (m, 3H); 8.299 (d, 1H). ¹³C NMR (CDCl₃, ppm) δ = 25.886; 28.631; 39.169;

50.729; 51.830; 59.026; 59.715; 121.485, 122.507; 136.132; 148.245; 158.371.

Synthesis of 3-((4-aminobutyl)(pyridin-2-ylmethyl)amino)propan-1-ol (6)

Yield: 1.73 g (73%). Anal. Calc. for $C_{13}H_{23}N_3O$ (MW: 237.18): C, 65.79; H, 9.77; N, 17.70. Found: 65.10; H, 9.45; N, 17.20%. IR (Nujol mull, cm^{-1}) 3360, 3288 ν (NH_2), 1591 ν ($C=N$)_{py}. 1H NMR ($CDCl_3$, ppm) δ = 1.324-1.503 (m, 6H); 2.275-2.454 (m, 6H); 3.505 (s, 4H); 4.538 (s, 3H); 6.960-7.455 (m, 3H); 8.298 (s, 1H). ^{13}C NMR ($CDCl_3$, ppm) δ = 23.495; 28.598; 29.624; 40.283; 51.612; 53.237; 59.436; 60.711, 121.218; 122.362; 135.758; 148.031, 158.747.

General synthesis of the complexes

A solution of 0.5 mmol of appropriate aldehyde, 2-hydroxy-3-methoxy-benzaldehyde (0.08 g, 0.5 mmol), 2-hydroxybenzaldehyde (0.06 g, 0.5 mmol), 3,5-di-tert-butyl-2-hydroxybenzaldehyde (0.117 g, 0.5 mmol) or 2-hydroxy-1-naphthaldehyde (0.086 g, 0.5 mmol) in methanol (50 ml) and 7 drops of $N(Et)_3$ were added dropwise to a refluxing solution of $Cu(ClO_4)_2 \cdot 6H_2O$ (0.184 g, 0.5 mmol) and the corresponding amine, **1** (0.098 g, 0.5 mmol) or **2** (0.105 g, 0.5 mmol) or **3** (0.112 g, 0.5 mmol) or **4** (0.105 g, 0.5 mmol) or **5** (0.112 g, 0.5 mmol) or **6** (0.119 g, 0.5 mmol) in the same solvent (50 mL). After refluxing for 12 h, the solution was concentrated in a rotary evaporator (**EXTREME CAUTION!**) at room temperature to ca. 5–10 mL. A small volume of diethyl ether was added slowly, producing powdery precipitate. The powdery $Cu(II)$ products were filtered off, washed with cold diethyl ether and dried under vacuum. Crystalline or powdery compounds were obtained by slow diffusion of diethyl ether vapor into a solution of these compounds in methanol or mixture of methanol and acetonitrile, as detailed below.

$[Cu^{II}L^{naph1}](ClO_4)$

Recrystallisation of the initial solid from mixture of CH_3OH and MeCN in a 5:1 ratio via slow vapour diffusion of Et_2O yields green powder (0.10 g, 79.8 %). Anal. Calc. for $C_{21}H_{22}ClCuN_3O_6$: C, 49.32; H, 4.34; N, 8.22. Found: C, 49.77; H, 4.55; N, 7.92%. IR (ATR, cm^{-1}) 1616 ν ($C=N$)_{imi}, 1604, 1458 ν ($C=N$)_{py} and ν ($C=C$), 1088, 620 ν (ClO_4). ESI-MS (MeOH, m/z^+): 411.1 $[Cu^{II}L^{naph1}]^+$. UV-Vis. $\{\lambda_{max}, nm (\epsilon_{max}, M^{-1} cm^{-1})\}$ in CH_3CN : 228 (21097), 390 (2572), 572 (116). Magnetic moment: $\mu_{eff} = 2.2$ B.M. [Gouy].

$[Cu^{II}L^{naph2}](ClO_4)$

Recrystallisation of the initial solid from CH_3OH via slow vapour diffusion of Et_2O yields green crystals (0.11 g, 83.7%). Anal. Calc. for $C_{22}H_{24}ClCuN_3O_6$: C, 50.29; H, 4.60; N, 8.00. Found: C, 50.22; H, 4.49; N, 7.97%. IR (ATR, cm^{-1}) 1616 ν ($C=N$)_{imi}, 1449 ν ($C=N$) and ν ($C=C$), 1088, 619 ν (ClO_4). ESI-MS (MeOH, m/z^+): 425.1 $[Cu^{II}L^{naph2}]^+$, 851.2 $([Cu^{II}L^{naph2}]_2+H)^+$, 949.2 $([Cu^{II}L^{naph2}]_2)ClO_4$. UV-Vis. $\{\lambda_{max}, nm (\epsilon_{max}, M^{-1} cm^{-1})\}$ in CH_3CN : 298 (17419), 387 (6369), 583 (141). Magnetic moment: $\mu_{eff} = 1.72$ B.M. [Gouy].

$[Cu^{II}L^{H3}](ClO_4)$

Recrystallisation of the initial solid from CH_3OH via slow vapour diffusion of Et_2O yields green crystals (0.08 g, 62 %). Anal. Calc. for $C_{19}H_{24}ClCuN_3O_6$: C, 46.63; H, 4.94; N, 8.59. Found: C, 46.62; H, 5.12; N, 8.39%. IR (ATR, cm^{-1}) 1619 ν ($C=N$)_{imi}, 1450 ν ($C=C$)_{py}, 1080, 620 ν (ClO_4). ESI-MS (MeOH, m/z^+): 389.1 $[Cu^{II}L^{H3}]^+$, 777.2 $([Cu^{II}L^{H3}]_2-H)^+$, 879.2

$([Cu^{II}L^{H3}]_2+2H)ClO_4^+$. UV-Vis. $\{\lambda_{max}, nm (\epsilon_{max}, M^{-1} cm^{-1})\}$ in CH_3CN : 224 (137236), 272 (25701), 374 (1377), 463 (314.12), 612 (128.46), 761 (76.53). Magnetic moment: $\mu_{eff} = 1.84$ B.M. [Gouy].

$[Cu^{II}L^{OMe3}](ClO_4)$

Recrystallisation of the initial solid from mixture of CH_3OH and MeCN in a 1:1 ratio via slow vapour diffusion of Et_2O yields green crystals (0.10 g, 80 %). Anal. Calc. for $C_{20}H_{26}ClCuN_3O_7$: C, 46.25; H, 5.05; N, 8.09. Found: C, 45.39; H, 5.29; N, 7.72%. IR (ATR, cm^{-1}): 1615 ν ($C=N$)_{imi}, 1600, 1454 ν ($C=N$)_{py} and ν ($C=C$), 1078, 621 ν (ClO_4). ESI-MS (MeOH, m/z^+): 419.1 $[Cu^{II}L^{OMe3}]^+$, 837.3 $([Cu^{II}L^{OMe3}]_2-H)^+$, 939.2 $([Cu^{II}L^{OMe3}]_2+2H)ClO_4^+$. UV-Vis. $\{\lambda_{max}, nm (\epsilon_{max}, M^{-1} cm^{-1})\}$ in CH_3CN : 238 (31324), 281 (18414), 384 (2537), 483 (303.65), 602 (133.7), 781 (94). Magnetic moment: $\mu_{eff} = 2$ B.M. [Gouy].

$[Cu^{II}L^{tBu3}](ClO_4)$

Recrystallisation of the initial solid from CH_3OH via slow vapour diffusion of Et_2O yields green powder (0.11 g, 73 %). Anal. Calc. for $C_{27}H_{40}ClCuN_3O_6$: C, 53.90; H, 6.70; N, 6.98. Found: C, 53.46; H, 6.63; N, 7.32%. IR (ATR, cm^{-1}): 1617 ν ($C=N$)_{imi}, 1441 ν ($C=C$), 1085, 622 ν (ClO_4). ESI-MS (MeOH, m/z^+): 501.2 $[Cu^{II}L^{tBu3}]^+$, 1001.5 $([Cu^{II}L^{tBu3}]_2-H)^+$, 1103.4 $([Cu^{II}L^{tBu3}]_2+2H)ClO_4^+$. UV-Vis. $\{\lambda_{max}, nm (\epsilon_{max}, M^{-1} cm^{-1})\}$ in CH_3CN : 228 (15389), 247 (14363.4), 279 (9711.6), 320 (3988), 381 (3323), 486 (122), 633 (121), 819 (60). Magnetic moment: $\mu_{eff} = 1.88$ B.M. [Gouy].

$[Cu^{II}L^{naph3}](ClO_4) \cdot 0.25 CH_3OH$

Recrystallisation of the initial solid from mixture of CH_3OH and CH_3CN in a 2:1 ratio via slow vapour diffusion of Et_2O yields green powder (0.09 g, 68 %). Anal. Calc. for $C_{23.25}H_{27}ClCuN_3O_{6.25}$: C, 51.01; H, 4.97; N, 7.68. Found: C, 51.2; H, 4.92; N, 7.73%. IR (ATR, cm^{-1}) 1615 ν ($C=N$)_{imi}, 1604, 1447 ν ($C=N$)_{py} and ν ($C=C$), 1079, 620 ν (ClO_4). ESI-MS (MeOH, m/z^+): 439.1 $[Cu^{II}L^{naph3}]^+$, 879.3 $([Cu^{II}L^{naph3}]_2+H)^+$, 979.2 $([Cu^{II}L^{naph3}]_2+2H)ClO_4^+$. UV-Vis. $\{\lambda_{max}, nm (\epsilon_{max}, M^{-1} cm^{-1})\}$ in CH_3CN : 238 (35335), 311 (17908), 398 (6036), 485 (sh), 600 (157), 770 (98). Magnetic moment: $\mu_{eff} = 2.01$ B.M. [Gouy].

$[Cu^{II}L^{H4}](ClO_4)$

Recrystallisation of the initial solid from a mixture of CH_3OH and CH_3CN in a 1:1 ratio via vapour diffusion of Et_2O yields green crystals (0.178 g, 75 %). Anal. Calc. for $C_{18}H_{22}ClCuN_3O_6$: C, 45.48; H, 4.66; N, 8.84. Found: C, 45.42; H, 4.93; N, 9.02%. IR (ATR, cm^{-1}): 1632 ν ($C=N$)_{imi}, 1600, 1445 ν ($C=N$)_{py} and ν ($C=C$), 1071, 619 ν (ClO_4). ESI-MS (MeOH, m/z^+): 375.1 $[Cu^{II}L^{H4}]^+$. UV-Vis $\{\lambda_{max}, nm (\epsilon_{max}, M^{-1} cm^{-1})\}$ in CH_3CN : 222 (18271), 244 (17469), 266 (14079), 371 (3402), 587 (169). Magnetic moment: $\mu_{eff} = 1.82$ B.M. [Gouy].

$[Cu^{II}L^{OMe4}](ClO_4)$

Recrystallisation of this solid from CH_3OH via slow vapour diffusion of Et_2O yields green crystals (0.095 g, 75 %). Anal. Calc. for $C_{19}H_{24}ClCuN_3O_7$: C, 45.15; H, 4.79; N, 8.31. Found: C, 45.29; H, 4.60; N, 8.40%. IR (ATR, cm^{-1}): 1622 ν ($C=N$)_{imi}, 1444 ν ($C=N$)_{py} and ν ($C=C$), 1068, 620 ν (ClO_4). ESI-MS (MeOH, m/z^+): 405.1 $[Cu^{II}L^{OMe4}]^+$. UV-Vis. $\{\lambda_{max}, nm (\epsilon_{max}, M^{-1} cm^{-1})\}$ in CH_3CN : 205 (22476), 240 (17281), 270 (12011), 382 (2324), 575 (174). Magnetic moment: $\mu_{eff} = 1.90$ B.M. [Gouy].

$[Cu^{II}L^{tBu4}](ClO_4) \cdot 0.1CH_3OH$

Recrystallisation of the initial solid from CH_3OH via slow vapour diffusion of Et_2O yields green powder (0.115 g, 78 %). Anal. Calc. for $C_{26.1}H_{38.4}ClCuN_3O_{6.1}$: C, 53.06; H, 6.55; N, 7.11. Found: C, 53.16; H, 6.63; N, 7.02%. IR (ATR, cm^{-1}): 1629 ν (C=N)_{imi}; 1612, 1462 ν (C=N)_{py} and ν (C=C), 1070, 620 ν (ClO_4). ESI-MS (MeOH, m/z^+): 487.2 $[Cu^{II}L^{Bu4}]^+$. UV-Vis. $\{\lambda_{max}, nm (\epsilon_{max}, M^{-1} cm^{-1})\}$ in CH_3CN : 227 (17049), 248 (14636), 274 (10800), 383 (3105), 630 (155). Magnetic moment: $\mu_{eff} = 1.95$ B.M. [Gouy].

$[Cu^{II}L^{naph4}](ClO_4)$

Recrystallisation of the initial solid from mixture of CH_3OH and CH_3CN in a 3:1 ratio via slow vapour diffusion of Et_2O yields green powder (0.191 g, 73 %). Anal. Calc. for $C_{22}H_{24}ClCuN_3O_6$: C, 50.29; H, 4.60; N, 8.00. Found: C, 50.67; H, 4.72; N, 7.73%. IR (ATR, cm^{-1}): 1618 ν (C=N)_{imi}; 1607, 1437 ν (C=N)_{py} and ν (C=C), 1072, 619 ν (ClO_4). ESI-MS (MeOH, m/z^+): 425.1 $[Cu^{II}L^{naph4}]^+$, 951.2 $([Cu^{II}L^{naph4}]_2ClO_4+2H)^+$. UV-Vis. $\{\lambda_{max}, nm (\epsilon_{max}, M^{-1} cm^{-1})\}$ in CH_3CN : 226 (27244), 237 (sh), 248 (sh), 287 (10913), 313 (8927), 383 (4194), 574 (162). Magnetic moment: $\mu_{eff} = 1.86$ B.M. [Gouy].

$[Cu^{II}L^{H5}]_2(ClO_4)_2$

Recrystallisation of the initial solid from mixture of CH_3CN and CH_3OH in a 5:1 ratio via vapour diffusion of Et_2O yields green crystals (0.342 g, 70 %). Anal. Calc. for $C_{38}H_{48}Cl_2Cu_2N_6O_{12}$: C, 46.63; H, 4.94; N, 8.59. Found: C, 46.72; H, 4.90; N, 9.01%. IR (KBr disc, cm^{-1}): 1620 ν (C=N)_{imi}; 1596, 1440 ν (C=N)_{py} and ν (C=C), 1069, 619 ν (ClO_4). ESI-MS (MeOH, m/z^+): 389.1 $[Cu^{II}L^{H5}]^+$, 879.1 $([Cu^{II}L^{H5}]_2ClO_4+2H)^+$. UV-Vis. $\{\lambda_{max}, nm (\epsilon_{max}, M^{-1} cm^{-1})\}$ in CH_3CN : 257 (6806), 305 (2924), 404 (379), 598 (92). Magnetic moment: $\mu_{eff} = 1.58$ B.M. per Cu atom [Gouy].

$[Cu^{II}L^{OMe5}]_2(ClO_4)_2$

Recrystallisation of the initial solid from mixture of CH_3OH and MeCN in a 5:1 ratio via slow vapour diffusion of Et_2O yields green powder (0.348 g, 67 %). Anal. Calc. for $C_{40}H_{52}Cl_2Cu_2N_6O_{14}$: C, 46.25; H, 5.05; N, 8.09. Found: C, 46.17; H, 5.25; N, 8.4%. IR (ATR, cm^{-1}): 1620 ν (C=N)_{imi}; 1444 ν (C=C), 1078, 620 ν (ClO_4). ESI-MS (MeOH, m/z^+): 419.1 $[Cu^{II}L^{OMe5}]^+$, 939.2 $([Cu^{II}L^{OMe5}]_2+2H)ClO_4^+$. UV-Vis. $\{\lambda_{max}, nm (\epsilon_{max}, M^{-1} cm^{-1})\}$ in CH_3CN : 258 (9704), 313 (3700), 406 (754), 587 (122). Magnetic moment: $\mu_{eff} = 1.52$ B.M. per Cu atom [Gouy].

$[Cu^{II}L^{tBu5}]_2(ClO_4)_2$

Recrystallisation of the initial solid from CH_3OH via slow vapour diffusion of Et_2O yields green crystals (0.189 g, 63 %). Anal. Calc. for $C_{54}H_{80}Cl_2Cu_2N_6O_{12}$: C, 53.90; H, 6.70; N, 6.98. Found: C, 53.65; H, 6.93; N, 7.22%. IR (ATR, cm^{-1}): 1624 ν (C=N)_{imi}; 1600, 1440 ν (C=N)_{py} and ν (C=C), 1074, 620 ν (ClO_4). ESI-MS (MeOH, m/z^+): 501.2 $[Cu^{II}L^{tBu5}]^+$. UV-Vis. $\{\lambda_{max}, nm (\epsilon_{max}, M^{-1} cm^{-1})\}$ in CH_3CN : 210 (127302), 229 (14206), 248 (13790), 275 (9945), 306 (4208), 383 (2838), 610 (166). Magnetic moment: $\mu_{eff} = 1.32$ B.M. per Cu atom [Gouy].

$[Cu^{II}L^{naph5}]_2(ClO_4)_2$

Recrystallisation of the initial solid from CH_3OH via slow vapour diffusion of Et_2O yields green powder (0.177 g, 66 %). Anal. Calc. for $C_{46}H_{52}Cl_2Cu_2N_6O_{12}$: C, 51.21; H, 4.86; N, 7.79. Found: C, 51.62; H, 4.93; N, 8.03%. IR (ATR, cm^{-1}): 1620 ν

(C=N)_{imi}; 1602, 1449 ν (C=N)_{py} and ν (C=C), 1079, 620 ν (ClO_4). ESI-MS (MeOH, m/z^+): 439.1 $[Cu^{II}L^{naph5}]^+$, 979.2 $([Cu^{II}L^{naph5}]_2+2H)ClO_4^+$. UV-Vis. $\{\lambda_{max}, nm (\epsilon_{max}, M^{-1} cm^{-1})\}$ in CH_3CN : 224 (36505), 322 (10751), 382 (4649), 402(sh), 599 (140). Magnetic moment: $\mu_{eff} = 1.66$ B.M. Cu atom [Gouy].

$[Cu^{II}L^{H6}](ClO_4)$

Recrystallisation of the initial solid from CH_3OH via slow vapour diffusion of Et_2O yields green powder (0.16 g, 65 %). Anal. Calc. for $C_{20}H_{26}ClCuN_3O_6$: C, 47.71; H, 5.21; N, 8.35. Found: C, 47.62; H, 5.42; N, 8.19%. IR (ATR, cm^{-1}) 1624 ν (C=N)_{imi}; 1446 ν (C=C), 1049, 620 ν (ClO_4). ESI-MS (MeOH, m/z^+): 403.1326 $[Cu^{II}L^{H6}]^+$. UV-Vis. $\{\lambda_{max}, nm (\epsilon_{max}, M^{-1} cm^{-1})\}$ in CH_3CN : 223 (49480), 273 (15334), 307 (5202), 371 (3433), 619 (136). Magnetic moment: $\mu_{eff} = 1.78$ B.M. [Gouy].

$[Cu^{II}L^{OMe6}](ClO_4) \cdot 0.25CH_3OH$

Recrystallisation of the initial solid from mixture of CH_3OH and MeCN in a 1:1 ratio via slow vapour diffusion of Et_2O yields green powder (0.18 g, 68 %). Anal. Calc. for $C_{21.25}H_{29}ClCuN_3O_{7.25}$: C, 47.14; H, 5.40; N, 7.76. Found: C, 47.24; H, 5.39; N, 7.72%. IR (ATR, cm^{-1}): 1615 ν (C=N)_{imi}; 1446 ν (C=C), 1074, 625 ν (ClO_4). ESI-MS (MeOH, m/z^+): 433.1411 $[Cu^{II}L^{OMe6}]^+$. UV-Vis. $\{\lambda_{max}, nm (\epsilon_{max}, M^{-1} cm^{-1})\}$ in CH_3CN : 204 (23919), 237 (21533), 281 (13442), 381 (3564), 594 (145). Magnetic moment: $\mu_{eff} = 1.74$ B.M. [Gouy].

$[Cu^{II}L^{tBu6}](ClO_4) \cdot 0.25H_2O$

Recrystallisation of the initial solid from CH_3OH via slow vapour diffusion of Et_2O yields green powder (0.19 g, 63 %). Anal. Calc. for $C_{28}H_{42.5}ClCuN_3O_{6.25}$: C, 54.23; H, 6.91; N, 6.78. Found: C, 54.23; H, 6.91; N, 6.78%. IR (ATR, cm^{-1}): 1613 ν (C=N)_{imi}; 1460 ν (C=C), 1081, 621 ν (ClO_4). ESI-MS (MeOH, m/z^+): 515.2532 $[Cu^{II}L^{tBu6}]^+$. UV-Vis. $\{\lambda_{max}, nm (\epsilon_{max}, M^{-1} cm^{-1})\}$ in CH_3CN : 203 (19536), 228 (15706), 248 (14105), 280 (9412), 328 (3974), 384 (3135), 507 (165), 621 (164). Magnetic moment: $\mu_{eff} = 1.92$ B.M. [Gouy].

$[Cu^{II}L^{naph6}](ClO_4)$

Recrystallisation of the initial solid from mixture of CH_3OH and CH_3CN in a 3:1 ratio via slow vapour diffusion of Et_2O yields green powder (0.19 g, 69 %). Anal. Calc. for $C_{24}H_{28}ClCuN_3O_6$: C, 52.08; H, 5.10; N, 7.59. Found: C, 52.42; H, 5.22; N, 7.33%. IR (ATR, cm^{-1}) 1622 ν (C=N)_{imi}; 1597, 1445 ν (C=N)_{py} and ν (C=C), 1051, 619 ν (ClO_4). ESI-MS (MeOH, m/z^+): 453.1437 $[Cu^{II}L^{naph6}]^+$. UV-Vis. $\{\lambda_{max}, nm (\epsilon_{max}, M^{-1} cm^{-1})\}$ in CH_3CN : 227 (26485), 235 (26573), 311 (12151), 383 (4209), 399 (4221), 588 (112). Magnetic moment: $\mu_{eff} = 2.02$ B.M. [Gouy].

Acknowledgements

We are grateful to the Faculty of Chemistry of Bu-Ali Sina University, Ministry of Science, Research and Technology of Iran, the University of Otago and the MacDiarmid Institute for Advanced Materials and Nanotechnology for financial support (PhD scholarship for SD), and Professor Sally Brooker for hosting MS for a 6-month research visit.

Notes and references

^a Faculty of Chemistry, Bu-Ali Sina University, Hamedan 65174, Iran; Fax: 98 8118 380709; Tel: 98 9188131117; email:

115 haskey1@yahoo.com

- ^b Department of Chemistry and the MacDiarmid Institute for Advanced Materials and Nanotechnology, University of Otago, PO Box 56, Dunedin 9054, New Zealand.
- ^c Department of Physics, Faculty of Science, Ankara University, TR-06100 Tandogan, Ankara, Turkey
- ^d Department of Physics, Arts and Sciences Faculty, Aksaray University, TR-68100, Aksaray, Turkey
- † Electronic Supplementary Information (ESI) available: [¹H]NMR, ¹³CNMR and IR spectra of amines (3-6) (Figures S1-S12), IR spectra of complexes (Figures S13-S30), Mass spectra of complexes (Figures S31-S48). Crystallographic data for the crystal structure analyses have been deposited with the Cambridge Crystallographic Data Centre, CCDC no. (968863), for [Cu^{II}L^{naph}](ClO₄), (968865), for [Cu^{II}L^{H3}](ClO₄), (1002225), for [Cu^{II}L^{OMe3}](ClO₄), (1002229), for [Cu^{II}L^{H4}](ClO₄) and (1002230), for [Cu^{II}L^{H5}]₂(ClO₄)₂. Copies of this information may be obtained free of charge from The Director, CCDC, 12 Union road, Cambridge, CB2 1EZ, UK (fax: +44 1223 336033; mail:deposit@ccdc.cam.ac.uk).]. See DOI: 10.1039/b000000x/
- (a) L.F. Szczepura, L.M. Witham and K.J. Takeuchi, *Coord. Chem. Rev.*, 1998, **174**, 5-32; (b) J.M. Baumeister, R. Alberto, K. Ortner, B. Spingler, P.A. Schubiger and T.A. Kaden, *J. Chem. Soc., Dalton Trans.*, 2002, 4143-4151; (c) I. Yoon, Y.W. Shin, J. Kim, K.-M. Park, S.B. Park and S.S. Lee, *Acta Crystallogr. C*, 2002, **58**, m165-m166; (d) K.S. Choi, D. Kang, J.-E. Lee, J. Seo and S.S. Lee, *Bull. Korean Chem. Soc.*, 2006, **27**, 747-754; (e) S. Chung, W. Kim, S.B. Park, I. Yoon, S.S. Lee and D.D. Sung, *J. Chem. Soc., Chem. Commun.*, 1997, 965-966; (f) S.S. Lee, J.M. Park, D.Y. Kim, J.H. Jung and M.H. Cho, *Chem. Lett.*, 1995, 1009-1010; (g) Y.-S. Xie, H. Jiang, X.-T. Liu, Z.-Y. Zhou, Q.-L. Liu and X.-L. Xu, *Collect. Czech. Chem. Commun.*, 2002, **67** 1647-1657.
 - S. Paul, A.K. Barik, R.J. Butcher, S.K. Kar, *Polyhedron*, 2000, **19**, 2661 – 2666.
 - L.R. Gahan, T.M. Donlevy and T.W. Hambley, *Inorg. Chem.*, 1990, **19**, 1451-1454.
 - A.M. Sargeson, *Pure Appl. Chem.*, 1984, **56**, 1603-1619.
 - K. Ziegler, *Methodes der Organischen Chemie*, Part 2, vol. 4, Houben-Weyl, Georg-Thieme-verlag, Stuttgart, 1955, p. 729.
 - J. Hunter, J. Nelson, C. Harding, M. McCann and V. McKee, *J. Chem. Soc., Chem. Commun.*, 1990, 1148-1151.
 - T.M. Garrett, T.J. McMurry, M.W. Hosseini, Z.E. Reyes, F.E. Hahn and K.N. Raymond, *J. Am. Chem. Soc.*, 1991, **113**, 2965-2977.
 - L. Busetto and V. Zanotti, *Inorg. Chim. Acta*, 2008, **361**, 3004-3011.
 - (a) R.L. Fanshawe and A.G. Blackman, *Inorg. Chem.*, 1995, **34**, 421-423; (b) A.M. Dittler-Klingemann and F.E. Hahn, *Inorg. Chem.*, 1996, **35**, 1996-1999; (c) A.M. Dittler-Klingemann, C. Orvig, F.E. Hahn, F. Thaler, C. Hubbard, R. van Eldik, S. Schindler and I. Fa'bia'n, *Inorg. Chem.*, 1996, **35**, 7798-7803.
 - C. Ochs, F.E. Hahn and R. Frohlich, *Chem. Eur. J.*, 2000, **6**, 2193-2199.
 - (a) B.A. Brennan, G. Alms, M.J. Nelson, L.T. Durney and R.G. Scarrow, *J. Am. Chem. Soc.*, 1996, **118**, 9194-9195; (b) R.G. Scarrow, B.S. Strickler, J.J. Ellison, S.C. Shoner, J.A. Kovacs, J.G. Cummings and M.J. Nelson, *J. Am. Chem. Soc.*, 1998, **120**, 9237-9245; (c) L. Heinrich, Y. Li, J. Vaissermann, G. Chottard and J.-C. Chottard, *Angew. Chem., Int. Ed. Engl.*, 1999, **38**, 3526-3528.
 - M.T. Werth, S.-F. Tang, G. Formicka, M. Zeppezauer, M.K. Johnson, *Inorg. Chem.*, 1995, **34**, 218-228.
 - (a) Y.-H. Chiu, G.J. Gabriel, J.W. Canary, *Inorg. Chem.*, 2005, **44**, 40-44; (b) G.J. Christian, A. Lobet, F. Maseras, *Inorg. Chem.*, 2010, **49**, 5977-5985.
 - H. Keypour, A.H. Jamshidi, M. Rezaeivala and L. Valencia, *Polyhedron*, 2013, **52**, 872-878.
 - M. Kalanithi, M. Rajarajan, P. Tharmaraj and C.D. Sheela, *Spectrochimica Acta Part A*, 2012, **87**, 155-162.
 - G. A. McLachlan, G. D. Fallon, R. L. Martin and L. Spiccia, *Inorg. Chem.*, 1995, **34**, 254-261.
 - S. J. Brudenell, L. Spiccia and E. R. T. Tiekink, *Inorg. Chem.*, 1996, **35**, 1974-1979; A. B. P. Lever, *Studies in physical and theoretical chemistry 33: Inorganic electronic spectroscopy*, Elsevier, Amsterdam, 1997.
 - B. Graham, M. T.W. Hearn, P. C. Junk, C. M. Kepert, F. E. Mabbs, B. Moubaraki, K. S. Murray and L. Spiccia, *Inorg. Chem.*, 2001, **40**, 1536-1543.
 - C. Ochs, F. E. Hahn and R. Fröhlich, *Eur. J. Inorg. Chem.*, 2001, **2001**, 2427-2436.
 - M. Du, Y.-M. Guo, S.-T. Chen, X.-H. Bu and J. Ribas, *Inorganica Chimica Acta*, 2003, **346**, 207-214.
 - S. Bhattacharyya, S.B. Kumar, S.K. Dutta, E.R.T. Tiekink and M. Chaudhury, *Inorg. Chem.*, 1996, **35**, 1967-1973.
 - B. Sarkar, M.S. Ray, Y.-Z. Li, Y. Song, A. Figuerola, E. Ruiz, J. Cirera, J. Cano and A. Ghosh, *Chem. Eur. J.*, 2007, **13**, 9297-9309.
 - B. Sarkar, S. Konar, C.J. Gomez-Garcia and A. Ghosh, *Inorg. Chem.*, 2008, **47**, 11611-11619.
 - B.J. Hathaway and A.A.G. Tomlinson, *Coord. Chem. Rev.*, 1970, **5**, 1-43.
 - M. Duggan, N. Ray, B. Hathaway, G. Tomlinson, P. Brint and K. Pelin, *J. Chem. Soc., Dalton Trans.*, 1980, 1342-1348.
 - N.J. Ray, L. Hulett, R. Sheahan and B. Hathaway, *J. Chem. Soc., Dalton Trans.*, 1981, 1463-1469.
 - E. Colacio, J.M. Domínguez-Vera, M. Gazi, R. Kivekäs, J.M. Moreno and A. Pajunen, *J. Chem. Soc., Dalton Trans.*, 2000, 505-509.
 - (a) M.J. Scott, S.C. Lee and R.H. Holm, *Inorg. Chem.*, 1994, **33**, 4651-4662.; (b) M.T. Gardner, G. Deinum, Y. Kim, G.T. Babcock, M.J. Scott and R.H. Holm, *Inorg. Chem.*, 1996, **35**, 6878-6884.; (c) R.T. Conley, *Infrared Spectroscopy*, Allyn & Bacon Inc., Boston, 1966; (d) K. Nakamoto, *Infrared and Raman Spectra of Inorganic and Coordination Compounds*; Part A and B, fifth ed., Wiley, New York, 1997.
 - N. Mondal, D.K. Dey, S. Mitra and V. Gramlich, *Polyhedron*, 2001, **20**, 607-613.
 - A. Bottcher, H. Elias, E. Jager, H. Lanfhelderora, M. Mazur, L. Mullor, H. Paulas, P. Pelikan, M. Rudolph and M. Valko, *Inorg. Chem.*, 1993, **32**, 4131-4138.
 - R.N. Patel, S.P. Rawat, M. Choudhary, V. P. Sondhiya, D. K. Patel, K.K. Shukla, D. K. Patel, Y. Singh and R. Pandey, *Inorganica Chimica Acta*, 2012, **392**, 283-291.
 - A. Kumar Sharma and R. Mukherjee, *Inorganica Chimica Acta*, 2008, **361**, 2768-2776.
 - E. V. Rybak-Akimova, A. Y. Nazarenko, L. Chen, P. W. Krieger, A. M. Herrera, V. V. Tarasov and P. D. Robinson, *Inorganica Chimica Acta*, 2001, **324**, 1-15.
 - N. J. Lundin, I. G. Hamilton and A. G. Blackman, *Polyhedron*, 2004, **23**, 97-102.
 - F. Tuna, G. I. Pascu, J.P. Sutter, M. Andruh, S. Golhen, J. Guillevic and H. Pritzkow, *Inorganica Chimica Acta*, 2003, **342**, 131-138.
 - B. Sreenivasulu, M. Vetrichelvan, F. Zhao, S. Gao and J. J. Vittal, *Eur. J. Inorg. Chem.*, 2005, **2005**, 4635-4645.
 - Y. Yahsi and H. Kara, *Inorganica Chimica Acta*, 2013, **397**, 110-116.
 - L. C. Nathan, J. E. Koehne, J. M. Gilmore, K. A. Hannibal, W. E. Dewhirst and T. D. Mai, *polyhedron*, 2003, **22**, 887-894.
 - A.W. Addison, T.N. Rao, J. Reedijk, J. van Rijn and G.C. Verschoor, *J. Chem. Soc., Dalton Trans.*, 1984, **7**, 1349-1356.
 - K.P. Maresca, G.H. Bonavia, J.W. Babich and J. Zubieta, *Inorg. Chim. Acta*, 1999, **284**, 252-257.

-
41. M. Li, A. Ellern and J.H. Espenson, *Inorg. Chem.*, 2005, **44**, 3690-3699.
42. J.F. Larrow and E.N. Jacobson, *J. Org. Chem.*, 1994, **59**, 1939-1942.
- 5 43. Bruker, APEX2, SAINT, SADABS and SHELXTL Bruker AXS Inc., Madison, Wisconsin, USA, 2012.
44. (a) G.M. Sheldrick, *Acta Crystallogr., Sect. A*, 1990, **46**, 467-473; (b) G.M. Sheldrick, *Methods Enzymol.*, 1997, **276**, 628-641.
- 10 45. G.M. Sheldrick and T.R. Schneider, *Methods Enzymol.*, 1997, **277**, 319-343.
46. G.M. Sheldrick, SHELXS97, University of Gottingen, Germany, 1997.
- 15 47. Y. Zhao, D.G. Truhlar, A new local density functional for main-group thermochemistry, transition metal bonding, thermochemical kinetics, and noncovalent interactions, *J. Phys. Chem. A*, 2006, **125**, 194101-194118.
48. M. J. Frisch, et al. Gaussian 09, revision A.02; Gaussian, Inc.:Wallingford, CT, 2009.
- 20
- 25
- 30
- 35
- 40
- 45